

**AFRL-IF-WP-TR-2004-1553**

**ADAPTIVE FILTERING IN THE  
WAVELET TRANSFORM DOMAIN  
VIA GENETIC ALGORITHMS**



**Frank Moore**

**University of Alaska at Anchorage  
Department of Mathematical Sciences  
CAS 154  
3211 Providence Drive  
Anchorage, AK 99501**

**Pat Marshall  
Eric Balster**

**Embedded Information Systems Engineering Branch (AFRL/IFTA)  
Advanced Systems Division  
Information Directorate  
Air Force Research Laboratory, Air Force Materiel Command  
Wright-Patterson Air Force Base, OH 45433-7334**

**AUGUST 2004**

**Final Report for 01 January 2004 – 31 May 2004**

**Approved for public release; distribution is unlimited.**

**STINFO FINAL REPORT**

**INFORMATION DIRECTORATE  
AIR FORCE RESEARCH LABORATORY  
AIR FORCE MATERIEL COMMAND  
WRIGHT-PATTERSON AIR FORCE BASE, OH 45433-7334**

# NOTICE

USING GOVERNMENT DRAWINGS, SPECIFICATIONS, OR OTHER DATA INCLUDED IN THIS DOCUMENT FOR ANY PURPOSE OTHER THAN GOVERNMENT PROCUREMENT DOES NOT IN ANY WAY OBLIGATE THE US GOVERNMENT. THE FACT THAT THE GOVERNMENT FORMULATED OR SUPPLIED THE DRAWINGS, SPECIFICATIONS, OR OTHER DATA DOES NOT LICENSE THE HOLDER OR ANY OTHER PERSON OR CORPORATION; OR CONVEY ANY RIGHTS OR PERMISSION TO MANUFACTURE, USE, OR SELL ANY PATENTED INVENTION THAT MAY RELATE TO THEM.

THIS REPORT IS RELEASABLE TO THE NATIONAL TECHNICAL INFORMATION SERVICE (NTIS). AT NTIS, IT WILL BE AVAILABLE TO THE GENERAL PUBLIC, INCLUDING FOREIGN NATIONALS.

THIS TECHNICAL REPORT HAS BEEN REVIEWED AND IS APPROVED FOR PUBLICATION.

/s/

---

PAT MARSHALL, Project Engineer/Team Leader  
Embedded Info Sys Engineering Branch  
Information Technology Division  
Information Directorate

/s/

---

AL SCARPELLI, Acting Chief  
Embedded Info Sys Engineering Branch  
Information Technology Division  
Information Directorate

Do not return copies of this report unless contractual obligations or notice on a specific document requires its return.

# REPORT DOCUMENTATION PAGE

*Form Approved*  
OMB No. 0704-0188

The public reporting burden for this collection of information is estimated to average 1 hour per response, including the time for reviewing instructions, searching existing data sources, gathering and maintaining the data needed, and completing and reviewing the collection of information. Send comments regarding this burden estimate or any other aspect of this collection of information, including suggestions for reducing this burden, to Department of Defense, Washington Headquarters Services, Directorate for Information Operations and Reports (0704-0188), 1215 Jefferson Davis Highway, Suite 1204, Arlington, VA 22202-4302. Respondents should be aware that notwithstanding any other provision of law, no person shall be subject to any penalty for failing to comply with a collection of information if it does not display a currently valid OMB control number. **PLEASE DO NOT RETURN YOUR FORM TO THE ABOVE ADDRESS.**

|   |                                    |                                     |   |   |  |
|---|------------------------------------|-------------------------------------|---|---|--|
| <b>1. REPORT DATE (DD-MM-YY)</b><br>August 2004   |                                    | <b>2. REPORT TYPE</b><br>Final      |   | <b>3. DATES COVERED (From - To)</b><br>01/01/2004 – 05/31/2004                      |  |
| <b>4. TITLE AND SUBTITLE</b><br>ADAPTIVE FILTERING IN THE WAVELET TRANSFORM DOMAIN VIA GENETIC ALGORITHMS   |                                    |                                     |   | <b>5a. CONTRACT NUMBER</b><br>FA8650-04-C-4205                                      |  |
|   |                                    |                                     |   | <b>5b. GRANT NUMBER</b>   |  |
|   |                                    |                                     |   | <b>5c. PROGRAM ELEMENT NUMBER</b><br>61102F   |  |
| <b>6. AUTHOR(S)</b><br>Frank Moore (University of Alaska at Anchorage)<br>Pat Marshall and Eric Balster (AFRL/IFTA)   |                                    |                                     |   | <b>5d. PROJECT NUMBER</b><br>WOGA   |  |
|   |                                    |                                     |   | <b>5e. TASK NUMBER</b><br>IF  |  |
|   |                                    |                                     |   | <b>5f. WORK UNIT NUMBER</b><br>TA   |  |
| <b>7. PERFORMING ORGANIZATION NAME(S) AND ADDRESS(ES)</b><br><br>University of Alaska at Anchorage<br>Department of Mathematical Sciences<br>CAS 154<br>3211 Providence Drive<br>Anchorage, AK 99501<br>-----<br>Embedded Information Systems Engineering Branch (AFRL/IFTA)<br>Advanced Systems Division<br>Information Directorate<br>Air Force Research Laboratory, Air Force Materiel Command<br>Wright-Patterson Air Force Base, OH 45433-7334   |                                    |                                     |   | <b>8. PERFORMING ORGANIZATION REPORT NUMBER</b>                                     |  |
| <b>9. SPONSORING/MONITORING AGENCY NAME(S) AND ADDRESS(ES)</b><br><br>Information Directorate<br>Air Force Research Laboratory<br>Air Force Materiel Command<br>Wright-Patterson AFB, OH 45433-7334   |                                    |                                     |   | <b>10. SPONSORING/MONITORING AGENCY ACRONYM(S)</b><br>AFRL/IFTA                     |  |
|   |                                    |                                     |   | <b>11. SPONSORING/MONITORING AGENCY REPORT NUMBER(S)</b><br>AFRL-IF-WP-TR-2004-1553 |  |
| <b>12. DISTRIBUTION/AVAILABILITY STATEMENT</b><br>Approved for public release; distribution is unlimited.   |                                    |                                     |   |   |  |
| <b>13. SUPPLEMENTARY NOTES</b><br>Report contains color.  |                                    |                                     |   |   |  |
| <b>14. ABSTRACT</b><br>This report primarily addresses the problem of quantization noise since it is one of the very few processes that potentially eliminates valuable signal information. In a lossy compression system, the quantization step is totally responsible for information loss resulting in quality reduction of the reconstructed signal. For this effort, adaptive filtering techniques are utilized for modifying standard, "off-the-shelf," discrete wavelet transform (DWT) coefficients in the hopes that the differential errors between the original uncorrupted signal and the corrupted signal will be minimized. These results show that coefficients evolved by a genetic algorithm (GA) can indeed outperform standard wavelet coefficients for reconstruction of one- and two-dimensional data subjected to quantization. This approach consistently identified coefficient sets that reduced mean squared error (MSE) and improved peak signal-to-noise ratio (PSNR) for inverse DWTs. |                                    |                                     |   |   |  |
| <b>15. SUBJECT TERMS</b><br>Genetic algorithms, discrete wavelet algorithms, quantization noise.  |                                    |                                     |   |   |  |
| <b>16. SECURITY CLASSIFICATION OF:</b>  |                                    |                                     | <b>17. LIMITATION OF ABSTRACT:</b><br>SAR | <b>18. NUMBER OF PAGES</b><br>50  | <b>19a. NAME OF RESPONSIBLE PERSON (Monitor)</b><br>Pat Marshall<br><b>19b. TELEPHONE NUMBER (Include Area Code)</b><br>(937) 255-6548 x3586 |
| <b>a. REPORT</b><br>Unclassified  | <b>b. ABSTRACT</b><br>Unclassified | <b>c. THIS PAGE</b><br>Unclassified |   |   |  |

## 1. INTRODUCTION

Adaptive filtering is a very powerful technique that is currently used for many military and commercial applications. This technique allows one to change the control or interface as a function of the surrounding environment. The basic idea is to extract enough information from particular signals to create a plant/model that emulates the resultant output signal as close as possible. One of most common uses of this type of digital signal processing (DSP) is for signal identification. Figure 1 shows a very basic example of this type of system.

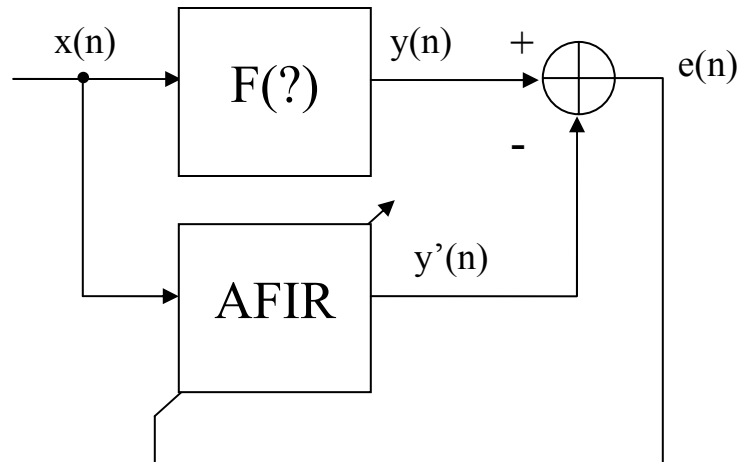


**Figure 1.** Basic system identification using adaptive filters block diagram.

The objective is to adjust the adaptive finite-impulse response (AFIR) filter's coefficients until the error signal  $e(n)$  is minimized to some predetermined level. This error signal is simply the magnitude difference sum of the unknown signal to be identified,  $y(n)$ , and its corresponding emulated signal  $y'(n)$ . Statistical algorithms such as the least mean square (LMS) algorithm, or deterministic approaches, such as the recursive least-squares (RLS), are usually employed inside the AFIR block shown in Figure 1 to adjust the finite-impulse response (FIR) coefficients.

Most adaptive filtering applications concentrate on optimizing the coefficients of FIR filters. Various iterative techniques (e.g., LMS using gradient descent) are employed to search for the optimal solution. In the current investigation, a new adaptive filtering method is introduced that uses GAs to modify the coefficient sets representing a selected wavelet to minimize the quantization error of the reconstructed signal. Unlike the signal identification process, however, this process requires access to all signal information. Consequently, this approach establishes a new method for using GAs to evolve sets of wavelet coefficients that outperform standard wavelet transforms used for reconstruction of one-dimensional (1-D) and two-dimensional (2-D) data subjected to quantization noise.

This research purposely chooses to concentrate all efforts on the lossy compression of signals, due to the fact that original signal information is permanently lost during the quantization process. This approach consistently identifies coefficient sets that significantly reduce MSE and improve PSNR for lossy compression systems based on the wavelet transform. A simple block diagram of our system is depicted in Figure 2.

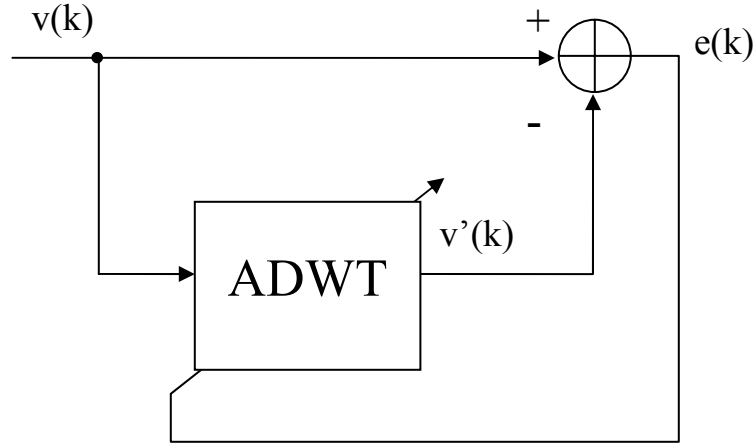


**Figure 2.** Basic block diagram of adaptive wavelet filtering system.

The main objective of the system shown in Figure 2 is to minimize the error signal,  $e(k)$ , which is a function of the magnitude differences between the original uncorrupted signal  $v(k)$  and the transformed, downsampled, quantized, dequantized, upsampled, and finally inverse transformed  $v(k)'$  signal. In this effort, the results of the error signal  $e(k)$  is used by a GA to adjust the filter coefficients of a preselected wavelet. The results of the GA process are then used to generate  $v(k)'$ . This entire process is contained within what is called the “Adaptive Discrete Wavelet Transform” (ADWT) plant shown in Figure 2.

Following the introduction, a background about previous DWT research is presented along with basic DWT and Quantization noise theory. The main research objective is then stated followed by a short demonstration of how sensitive the DWT reconstruction process is to changes in its filter coefficients. Then a brief introduction into basic GA theory is presented. Finally, the experimental results are presented followed by conclusions and proposed future research.

Note that, throughout this report, any reference to the wavelet forward and inverse transforms is termed as "standard" transforms such as the Harr and Daub4 wavelet transforms. Whereas the term “evolved” pertains only to the altered wavelet coefficients used during the inverse transform process.

## 2. BACKGROUND

The image processing research conducted at the AFRL/IFTA Reconfigurable Computing Laboratory has been successful in several areas. For example, several CAD programs have been developed to provide a means of efficiently evaluating various wavelet-based compression algorithms. This software permits the user to manually select standard wavelets for a particular application (e.g., SAR image compression). The hope is that the results are ultimately deemed acceptable for utilization in various unmanned aerial vehicle imaging systems. Once airborne, the transforms are to be used on-board the airframe to compress and transmit imagery to the remote ground station for viewing and evaluation.

The applications developed in this research effort use wavelet filters that have been previously discovered by other works such as that accomplished by, for example, Harr in 1920 and Daubechies in 1992. The wavelet selection criterion is traditionally a subjective decision based upon both the type of data to be processed and the type of processing. With a limited number of wavelet filters, it is unknown whether other filters may perform much better, depending upon the particular environment through which the system is operating and the mission to be accomplished. Furthermore, a previously selected wavelet may not work as well in a particular environment where other wavelets may be better suited. Thus, a chosen wavelet may only work satisfactorily for specific periods of time, and the wavelet may not be optimized when scenes change (e.g., from ground to air or ground to water). This problem is the main impetus behind the current research.

### 3. THE DISCRETE WAVELET TRANSFORM

Fourier analysis (Stein and Weiss 1971) is based upon the idea that all continuous signals may be represented by a sum of infinitely repeating sines and cosines. Fourier transforms and their variants [e.g., the Fast Fourier Transform (Cooley and Tukey 1965)] provide information about the frequencies present in a signal, but fail to describe where and when those frequencies occur in either time or space. In contrast, wavelets transform time-domain signals to a joint time-frequency domain. A wavelet transform convolves a given signal with particular instances of the wavelet at various time scales and positions. Since changes in frequency may be modeled by changing the time scale, and time changes may be modeled by shifting the position of the wavelet, wavelets allow us to represent both the frequencies within a given signal and the location of those frequencies. However, unlike the sinusoidal functions involved in the Fourier transform, wavelets exist only within finite intervals, and are zero-valued outside of those intervals.

The DWT is used to redistribute the energy of a given signal. The two main components of the classical DWT are (1) the scaling function  $\phi(t)$  and (2) the wavelet function  $\psi(t)$ , which are defined as follows:

$$\phi(t) = \sum_n h_n \phi(2t - n) \quad (1)$$

$$\psi(t) = \sum_n g_n \phi(2t - n) \quad (2)$$

where

$h_n$  = impulse response of the scaling filter,

$g_n$  = impulse response of the wavelet filter,

$n$  = denotes the scale and shift of these functions.

Moreover,  $h_n$  contains the set of filter coefficients corresponding to the projection of the basis functions for the low-pass filtering section of the DWT, and  $g_n$  contains filter coefficients corresponding to the projection of the basis functions for the high-pass filtering section of the DWT.

Once transformed, the analysis of signal input  $x(t)$  results in discrete sets of data in the wavelet domain.

The inverse DWT ( $DWT^{-1}$ ) is used to transform coefficients from the wavelet domain back into the original signal domain. In other words, the inverse transform produces the original signal  $x(t)$  from the wavelet and scaling coefficients.

$$x(t) = \sum_{k=-\infty}^{+\infty} \sum_{n=-\infty}^{+\infty} d_{k,n} \psi_{k,n}(t) \quad (3)$$

where

$$d_{k,n} = \int_{-\infty}^{+\infty} \psi_{k,n}^*(t) x(t) dt \quad (4)$$

A DWT perfectly describes a continuous-time signal  $x(t)$  using a countable set of coefficients. The DWT shown in Figure 3 is a multi-pass process that uses a scaling function and a wavelet function to separate the high-pass and low-pass information content of a given signal.

The low-pass sub-band produced by the previous transform is then subdivided into its own low and high sub-bands by the next level of the transform. Using the *multiresolution analysis* (MRA) technique (Mallat 1989), this process could be repeated as many times as the signal length can be divided by two (Walker 1999, p. 16); in practice, however, it is common to perform only a relatively small number of iterations (i.e., levels of decomposition), since nearly all of the energy of the decomposition coefficients is concentrated in the lower subbands (Rajoub 2002).

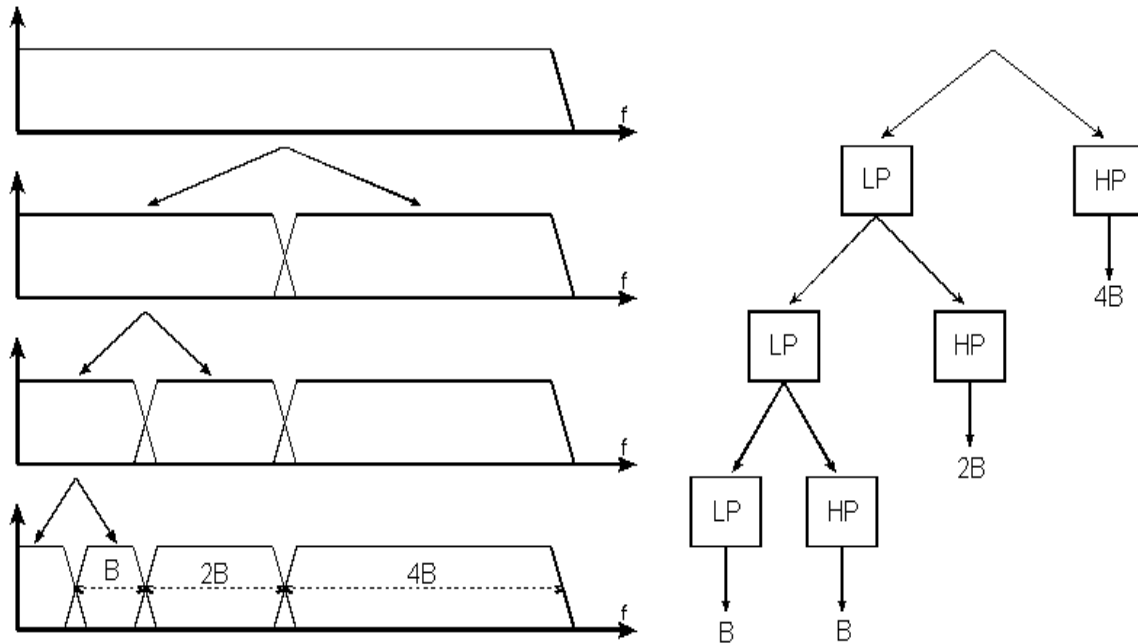


**Figure 3.** (Forward) DWT with Multi-resolution

Standard wavelets may be described by sets of coefficients (Daubechies 1992, p. 54-56), commonly named  $g$  and  $h$  for the high-pass and low-pass filters, respectively. For example, the Haar and Daubechies-4 (Daub4) wavelets are defined in Table 1.

**Table 1.** Mathematical Definitions for Haar and Daub4 Wavelets

| Haar  | Daub4   |
|---|---|
| $h = \left\{ \frac{1}{\sqrt{2}}, \frac{1}{\sqrt{2}} \right\}$ | $h = \left\{ \frac{\sqrt{2} * (1 + \sqrt{3})}{8}, \frac{\sqrt{2} * (3 + \sqrt{3})}{8}, \frac{\sqrt{2} * (3 - \sqrt{3})}{8}, \frac{\sqrt{2} * (1 - \sqrt{3})}{8} \right\}$ |
| $g(n) = -1^n h[P - n]$  | $g(n) = -1^n h[P - n]$  |

where  $n$  is the (spatial) position, and  $P$  is the filter length. ( $P = 2$  for the Haar wavelet and  $P = 4$  for the Daub4 wavelet.) Although Haar wavelets (Haar 1910) are the simplest wavelets to describe, Daubechies wavelets (Daubechies 1992) are more commonly used in certain applications. Figure 4 is a graphic illustration of the time-domain behavior of each of the wavelets defined in Table 1. Daub4 wavelets use filter banks (Vaidyanathan 1992) containing exactly four elements.

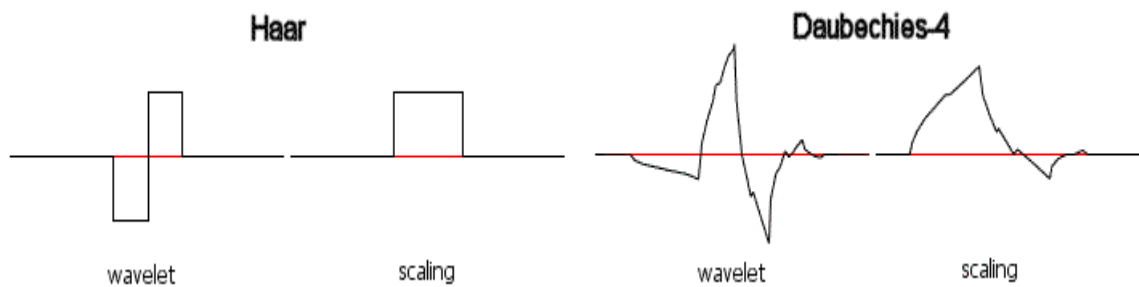


**Figure 4.** Time-Domain Representation of Wavelet and Scaling Function of Haar and Daub4 Wavelets

An N-stage 1-D DWT is depicted in Figure 5.

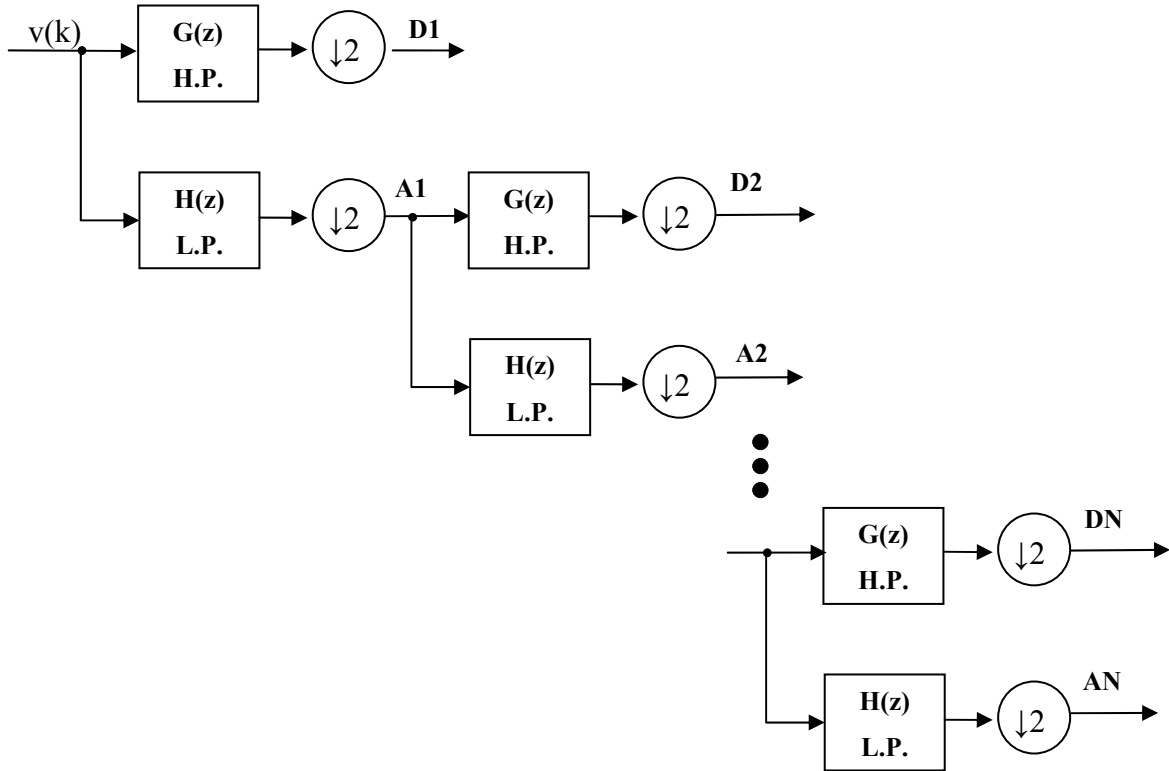


**Figure 5.** N-Stage, 1-D Analysis DWT Filter

A forward wavelet transform can be performed via matrix multiplication. As an illustrative example, consider a 1-D scenario that uses a Daub4 filter and an input signal  $x$  of length eight. If the four vectors ( $a$  and  $d$ ) comprising the low-pass and high-pass sections are combined to make a single eight-row vector, then the following matrix product defines the forward DWT:

$$\begin{bmatrix} a(0) \\ a(1) \\ a(2) \\ a(3) \\ d(0) \\ d(1) \\ d(2) \\ d(3) \end{bmatrix} = \begin{bmatrix} h3 & h2 & h1 & h0 & 0 & 0 & 0 & 0 \\ 0 & 0 & h3 & h2 & h1 & h0 & 0 & 0 \\ 0 & 0 & 0 & 0 & h3 & h2 & h1 & h0 \\ h1 & h0 & 0 & 0 & 0 & 0 & h3 & h2 \\ g3 & g2 & g1 & g0 & 0 & 0 & 0 & 0 \\ 0 & 0 & g3 & g2 & g1 & g0 & 0 & 0 \\ 0 & 0 & 0 & 0 & g3 & g2 & g1 & g0 \\ g1 & g0 & 0 & 0 & 0 & 0 & g3 & g2 \end{bmatrix} \begin{bmatrix} x(0) \\ x(1) \\ x(2) \\ x(3) \\ x(4) \\ x(5) \\ x(6) \\ x(7) \end{bmatrix}$$

The equivalent C language algorithm that illustrates a single step of a 1-D forward DWT utilizing a Daub4 wavelet is as follows:

```

N = 8;
for (i = 0; i < (N/2); i++)
{
    a = (2i + 2) % N;
    b = (2i + 3) % N;
    a[i] = x[2i]*h[3] + x[2i+1]*h[2] + x[a]*h[1] + x[b]*h[0];
    d[i] = x[2i]*g[3] + x[2i+1]*g[2] + x[a]*g[1] + x[b]*g[0];
}

```

where  $x$  is the input signal,  $N$  is the length of that signal,  $g$  is the wavelet filter, and  $h$  is the scaling filter. The resulting high-pass ( $d$ ) and low-pass ( $a$ ) signals each contain  $N/2$  values. Additional steps repeat this process using only the low-pass data; for each additional step,  $n$  will be half its value from the previous step.

An  $n$ -stage 1-D inverse DWT<sup>-1</sup> is depicted in Figure 6.

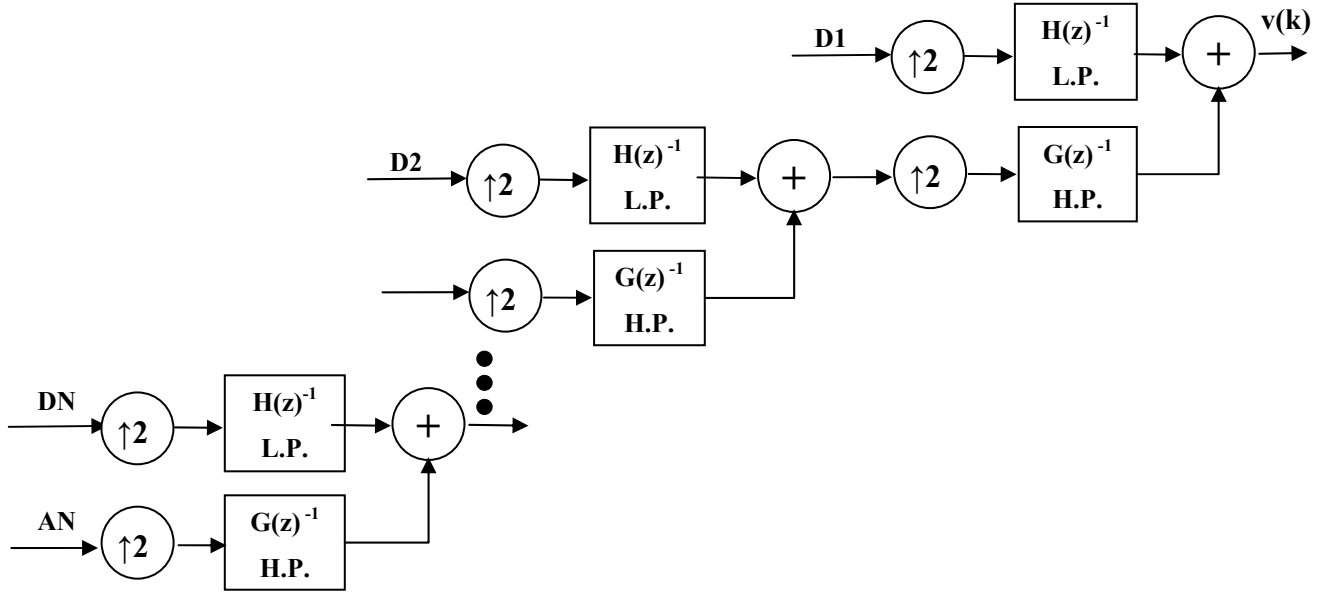


**Figure 6.** N-Stage, 1-D Analysis Synthesis DWT<sup>-1</sup> Filter.

Similarly, the 1-D inverse DWT<sup>-1</sup> for our previous matrix example can be expressed as follows:

$$\begin{bmatrix} x(0) \\ x(1) \\ x(2) \\ x(3) \\ x(4) \\ x(5) \\ x(6) \\ x(7) \end{bmatrix} = \begin{bmatrix} h3 & 0 & 0 & h1 & g3 & 0 & 0 & g1 \\ h2 & 0 & 0 & h0 & g2 & 0 & 0 & g0 \\ h1 & h3 & 0 & 0 & g1 & g3 & 0 & 0 \\ h0 & h2 & 0 & 0 & g0 & g2 & 0 & 0 \\ 0 & h1 & h3 & 0 & 0 & g1 & g3 & 0 \\ 0 & h0 & h2 & 0 & 0 & g0 & g2 & 0 \\ 0 & 0 & h1 & h3 & 0 & 0 & g1 & g3 \\ 0 & 0 & h0 & h2 & 0 & 0 & g0 & g2 \end{bmatrix} \begin{bmatrix} a(0) \\ a(1) \\ a(2) \\ a(3) \\ d(0) \\ d(1) \\ d(2) \\ d(3) \end{bmatrix}$$

The following C language algorithm describes the 1-D *inverse* DWT<sup>-1</sup> for a Daub4 wavelet used in this matrix example:

```

N = 8;
for (i = 0; i < (N/2); i++)
{
    x[2i ] = a[i-1]*h[1] + a[i]*h[3] + d[N-1]*g[1] + d[N]*g[3];
    x[2i+1] = a[N-1]*h[0] + a[N]*h[2] + d[N-1]*g[0] + d[N]*g[2];
}

```

where  $x$  is the reconstructed output signal,  $N$  is the discrete length of that signal,  $g$  is the wavelet filter, and  $h$  is the scaling filter. The resulting high-pass ( $d$ ) and low-pass ( $a$ ) signals each contain  $N/2$  values. Additional steps repeat this process using only the low-pass data. For each additional step,  $N$  will be half its value from the previous step. It is important to note that a separable 2-D transform on, for example, visible images is accomplished by performing a 1-D transform on each row, followed by a 1-D transform on each column.

Lossy Wavelet-based compression methods are capable of much greater compression gain than can be achieved by lossless methods. However, a fundamental theorem from information theory (Shannon and Weaver 1964) places limits on the amount of compression that can be achieved by a lossless encoding technique. This additional compression comes at the price of introducing inaccuracies into the reconstructed signal (Walker 1999, p. 19). As such, wavelets (Graps 1995) provide a powerful technique for efficiently representing large amounts of data.

Note that “perfect reconstruction” of 1-D signals or 2-D images is only possible due to the properties of the *orthonormal basis vectors* used by the DWT process. Examples of orthogonal functions are trigonometric and exponential functions (trigonometric functions are currently being used for DCT-based compression methods such as JPEG).

Two or more vectors are orthonormal if and only if their total dot product is zero, i.e., each vector must have a zero component in the direction of every other vector. Assume that we are working in 2-D rectangular space and we define that space with two unit basis vectors:

$$\bar{a}_x, \bar{a}_y \quad (5)$$

The two unit vectors form an orthonormal set if, for all  $x, y$ :

$$\bar{a}_x \bullet \bar{a}_y = 0 \quad (6)$$

#### 4. QUANTIZATION NOISE

For DSP applications, quantization of data is an absolute necessity through analog-to-digital conversion. In these situations, quantization noise occurs when the number of bits used is insufficient for representing the full dynamic range of the signal. In lossy compression methods, quantization is used to decrease the dynamic range of the signal reducing the amount of data necessary to represent the signal. For example, a 32-bit signed integer (whose value may range from  $-2^{31}$  to  $+2^{31} - 1$ ) may be quantized to 16-bit values (ranging from  $-2^{15}$  to  $+2^{15} - 1$ ); in this case, quantization reduces the amount of information of the resulting signal up to a factor of 65536. In effect, the information contained in the least significant 16 bits of the original signal is lost. Figure 7 shows a 1-D example of this process.

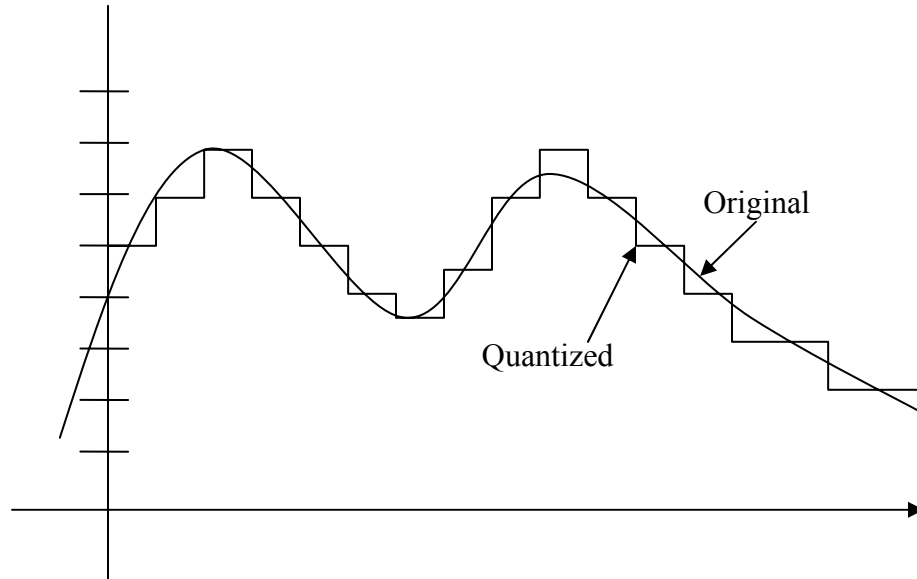


**Figure 7.** Quantization example.

As can be seen, the staircase function resulting from quantization is not equivalent to the original continuous function. The difference between the original function's magnitude and the quantized one at each discrete point is defined as the *quantization error*.

Quantization usually involves one of two processes: either (1) truncation or (2) rounding. To truncate, one simply discards bits to the right of the least significant bit. To round, one looks at the value of the most significant bit of that portion of the signal which is being eliminated; the value of the remaining signal is incremented if and only if this bit is set. Quantization is not an additive process and in fact discards (sometimes valuable) information. In addition, quantization is inherently a non-linear process which makes accurate reconstruction of the original signal more difficult.

Haar, Daubechies, and other families of wavelets have certain desirable properties that make them very useful for image compression. First, these wavelets conserve energy: that is, the total amount of energy from the original signal is retained in the wavelet domain (Walker 1999, pp. 6-7, 9, 38-40). Second, these wavelets redistribute the energy from the original signal, such that nearly all of that energy is stored in the first trend subsignal,  $\mathbf{a}^1$ ; most of the remaining values of the wavelet coefficients will be insignificant, and may be eliminated without significant loss of information (Saha 2000).

In a typical wavelet application, a signal is forward wavelet transformed by a wavelet and is then quantized (Q) immediately prior to an encoding step (E) for compression. The results are then transmitted over a wire, air, etc, medium. On the receiving end, the incoming signal is decoded (D), dequantized ( $Q^{-1}$ ) and then an inverse wavelet transform is executed in an attempt to reconstruct the original signal as accurately as possible. The inverse transform reconstructs an approximation of the original signal (Burrus, Gopinath, and Guo 1998, pp. 206-207). A simple block-diagram depiction of this process is shown in Figure 8 that is used in a real-world system.

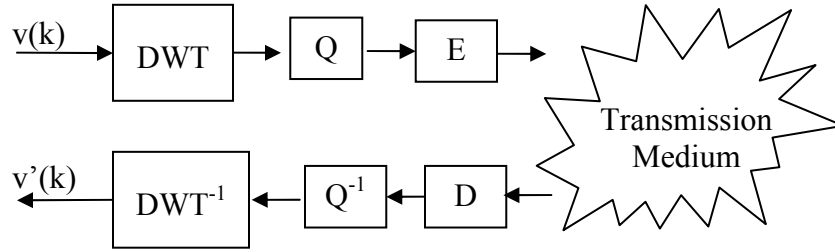


**Figure 8.** 1-D Reconstruction DWT Filter with Quantization

When the inverse wavelet transform is performed, loss of information due to quantization errors may cause the resulting decompressed signal to differ measurably from the original signal. This difference may be expressed as a mean-squared error (MSE) between the original  $k$ -size signal  $v(k)$  and the decompressed  $k$ -size signal  $v'(k)$ :

$$MSE = \frac{1}{N} \sum_n (v[n] - v'[n])^2 \quad (7)$$

where

$$N = \text{length of vector } v.$$

Note that MSE increases in proportion to the degree of quantization introduced into the transmitted signal.

For most image-processing applications, MSE is the figure-of-merit of choice for quantifying the amount of quantization noise, which in turn becomes one of the most important factors that quantifies the quality of the reconstructed signal. In this paper, MSE is utilized to quantify quantization noise resulting of a discrete mapping of an arbitrary array of image data points onto a smaller size/range of image data points. As mentioned previously, quantization noise is one of the few non-linear processes which deliberately discards signal information which automatically makes it much more difficult to reconstruct the original signal. This statement is worth repeating since the population-based search properties of GAs have proven to be particularly effective in identifying optimized solutions to various non-linear processes.

## 5. RESEARCH OBJECTIVE: MINIMIZING QUANTIZATION NOISE

For image compression, the main objective is to reduce the amount of data to be transmitted. This is especially true for bandwidth-limited systems. Unfortunately, on the receiving end, the image can never be perfectly reconstructed using standard wavelet inverse transforms. The required information is already gone. One can only hope to adjust the resultant image in some way as to minimize the MSE.

As mentioned previously, adaptive filtering techniques are utilized for optimizing filter coefficients of some plant/model until the resultant output signal emulates the original signal as close as

possible. Specifically, *can Adaptive Filter Techniques compensate for information loss due to quantization?* This observation raises the key question to be addressed in this research:

*Is it possible to use a GA to “adaptively” evolve a set of optimized g and h coefficients for an inverse wavelet transform, such that the MSE of images reconstructed by this inverse transform is significantly less than the mean squared error of images reconstructed by the standard wavelet inverse transform?*

As such, the purpose of this investigation is to determine whether a GA (Goldberg 1989) can be used to automatically optimize sets of wavelet coefficients that outperform standard wavelets for such applications as (1-D) vector reconstruction (Bradley, Brislawn, and Hopper 1994) and (2-D) image reconstruction (Saha 2000).

## 6. SENSITIVITY ANALYSIS OF ORTHONORMAL BASIS FUNCTIONS

Before a discussion of the actual GA/Wavelet modification experiments, a short demonstration on how changes to some filter coefficients impacts the signal reconstruction process. Perfectly reconstructed 1-D signals or 2-D images are only possible due to the properties of the orthonormal basis vectors used in the DWT. For the 1-D case, assume that a set of vectors spans some vector space such as time. Figure 9 details how this experiment will take place. The filter coefficients are used for the inverse transform  $DWT^{-1}$ .

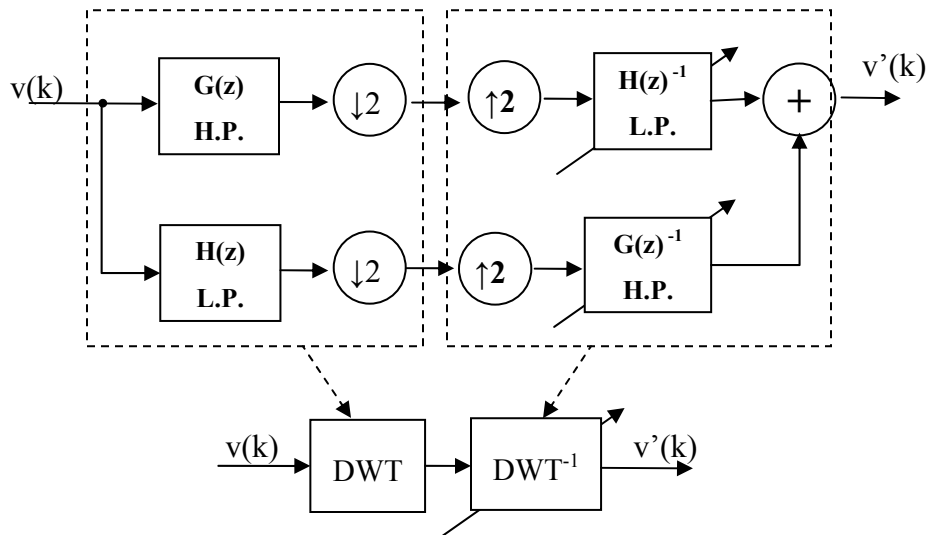


**Figure 9.** 1-D Reconstruction DWT Filter with Quantization

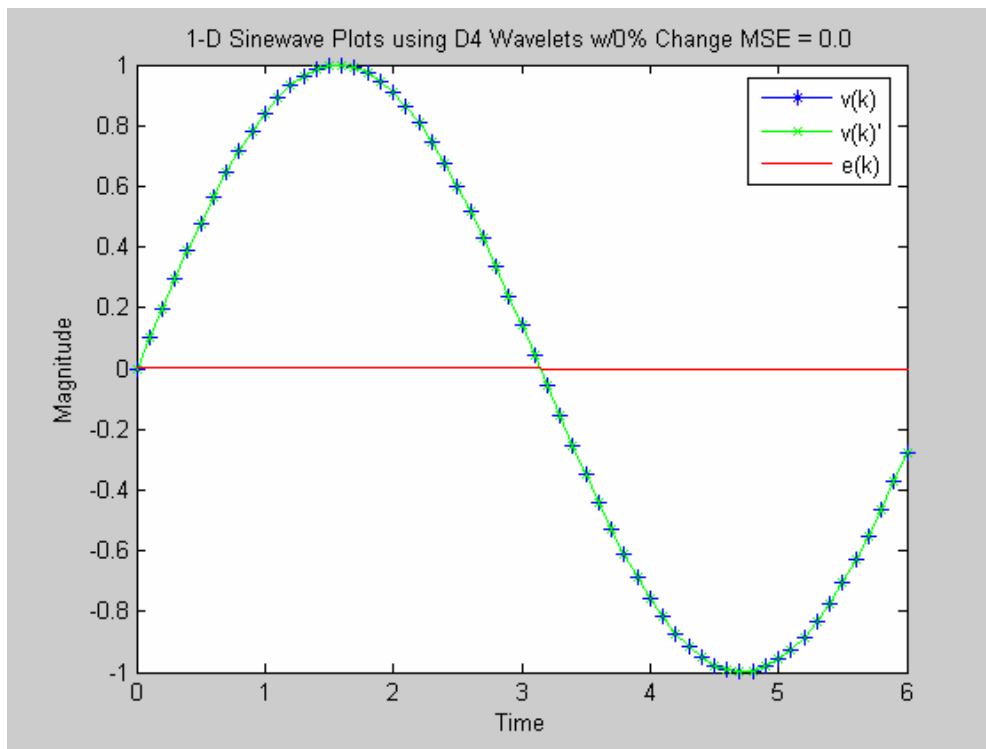
The adjustable arrow through the  $DWT^{-1}$  in Figure 9 represents the percentage change to the original Daub4 inverse transform filter coefficients. The Daub4 filter coefficients used for the analysis and synthesis functions are shown in Table 2.

**Table 2.** Original Discrete Daub4 Wavelets

| Filter # | Coefficients |          |         |          | Change (%) |
|----------|--------------|----------|---------|----------|------------|
| h1       | -0.12941     | 0.22414  | 0.83652 | 0.48296  | 0          |
| g1       | -0.4829      | 0.83652  | -0.2241 | -0.12941 | 0          |
| h2       | 0.48296      | 0.83652  | 0.22414 | -0.12941 | 0          |
| g2       | -0.12941     | -0.22414 | 0.83652 | -0.48296 | 0          |

The h1 and g1 coefficients are used respectively in the  $H(z)$  and  $G(z)$  forward transform blocks shown previously in Figure 9. The h2 and g2 coefficients are used respectively in the  $H(z)^{-1}$  and  $G(z)^{-1}$  reverse transform blocks shown previously in Figure 9.

A demonstration of the power of perfect reconstruction with 0% change to the  $DWT^{-1}$  coefficients will now be demonstrated. The test input signal “ $v(k)$ ” will be a 1-D sine-wave in this case. The  $v(k)$  signal is transformed using the “h1 and g1” filter coefficients shown in Table 2 and then downsampled as shown previously in Figure 9. The resultant signal is then upsampled and inverse-transformed using the “h2 and g2” coefficients shown in Table 2 above. The results of this process are shown in Figure 10.

**Figure 10.** 1-D Sine Wave Perfect Reconstruction Daub4 Filter without Quantization

In Figure 10, the input signal’s symbol is “ $v(k)$ ” and the output symbol stands is “ $v(k)'$ ”. The “ $e(k)$ ” in this case is simply the magnitude error difference between the two signals at a specific point in time. Specifically “ $e(k)$ ” is defined by:

$$e(k) = v(k) - v(k)' \quad (8)$$

Now, as a second experiment, the  $h_2$  and  $g_2$  filter coefficients are adjusted manually by 20% each as shown in Table 3 below. The choice of 20% is arbitrary and is for illustrative purposes only.

**Table 3.** 20% Change in Daub4 Wavelets

| Filter # | Coefficients |          |         |          | Change (%) |
|----------|--------------|----------|---------|----------|------------|
| h1       | -0.12941     | 0.22414  | 0.83652 | 0.48296  | 0          |
| g1       | -0.4829      | 0.83652  | -0.2241 | -0.12941 | 0          |
| h2       | 0.57956      | 1.0038   | 0.26897 | -0.10353 | 20         |
| g2       | -0.10353     | -0.17932 | 1.0038  | -0.38637 | 20         |

The results of the same reconstruction process is now shown in Figure 11.

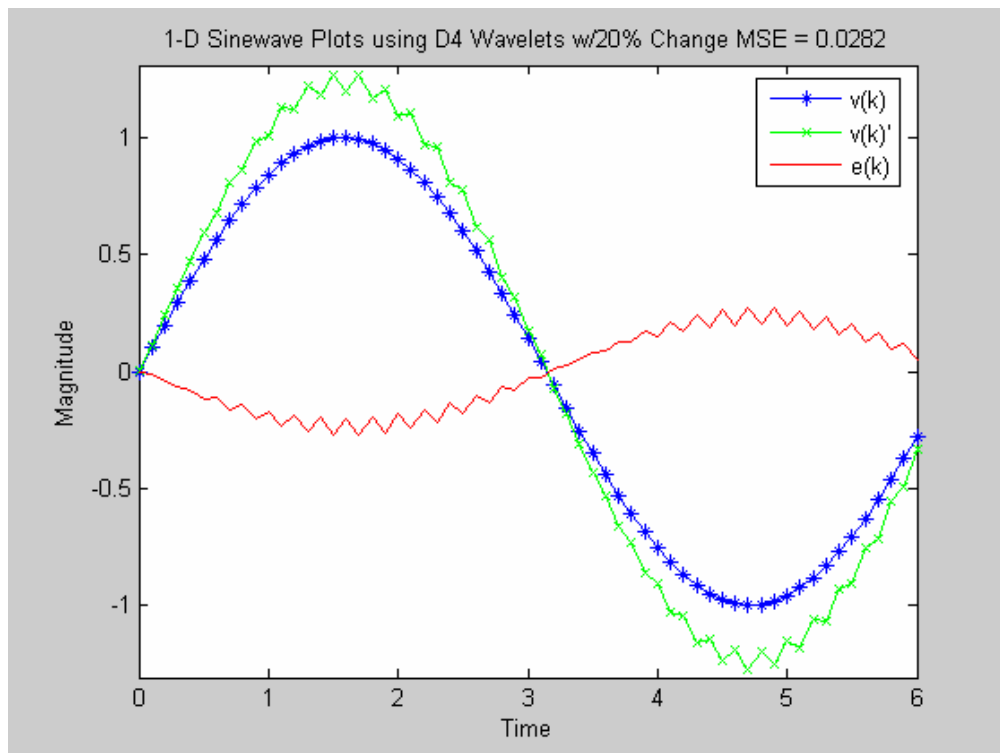


**Figure 11.** 1-D Sine Wave Daub4 Filter with 20% Change of  $h_2$  &  $g_2$  DWT Coefficients

The same process will now be repeated as another example but now with images. Figure 12 demonstrates the power of perfect reconstruction for images, with 0% change to the  $DWT^{-1}$  coefficients on the standard 256X256 “Barb” image. The Daub4 filter coefficients used for the sine wave analysis and synthesis functions are the same as what is shown in Table 2.



**Figure 12.** 2-D “Barb” Image using Daub4 Filter with 0% Change of  $h_2$  &  $g_2$  DWT Coefficients

Figure 13 shows the same image reconstructed with a 20% change in the  $h_2$  and  $g_2$  filter coefficients. The coefficients are shown in Table 3.



**Figure 13.** 2-D “Barb” Image with a 20% Change in Daub4  $h_2$  &  $g_2$  Wavelets

Note that there are a vast number of ways to adjust these filter coefficients. However, for demonstration purposes only it was decided to only adjust the filter coefficients in one direction (i.e., positive) with the same amount of magnitude (i.e., 20%). The main purpose of this section is to give the reader a flavor of what manually adjusting the filter coefficients of the DWT can do.

This short experiment highlights the fact that, even with the modification of the “h2” and “g2” filter coefficients, the resultant reconstructed 1-D and 2-D information can still be recognizable by the human eye. As a result, one may state the coefficients are quite “robust” which make them a very suitable to be used as variables in this adaptive information processing system.

## 7. THE GENETIC ALGORITHM

Optimization is a process by which the object is to “enhance” some parametric output of a system. Genetic Algorithms are one such process that uses evolution as its basic model to formulate various stochastic rules. The GA developed for this research effort closely follows a standard GA (Holland 1975), employing fitness-driven selection, crossover, and mutation operators to create each new generation of candidate solutions. The main components to most standard GAs are shown below in Figure 14 below.

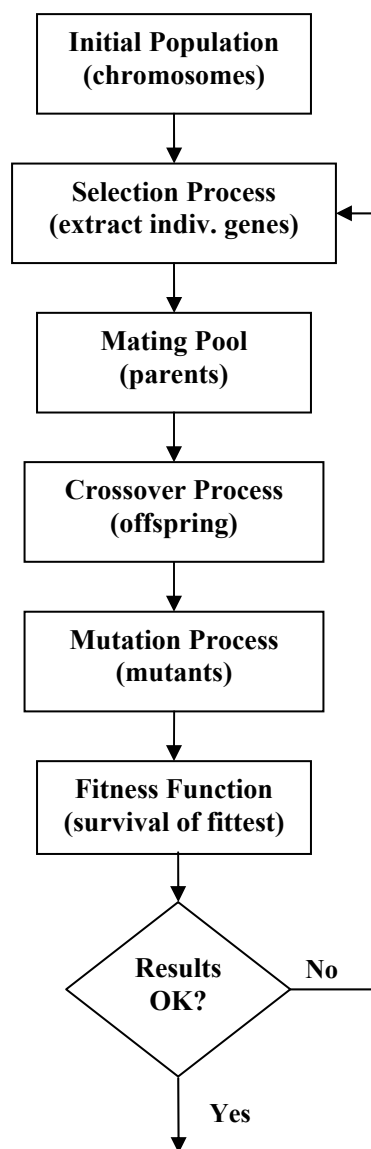


**Figure 14.** Diagram of a basic GA

The initial population is usually generated by some random number generator algorithm to create an initial array of populations. The selection, mating, and crossover processes are then used to decide which parts (i.e., genes) of which parents, from the current population, are to be used to create the new genes of the offspring. However, sometimes the GA may sometimes find itself “stuck” in a local minimum. In situations like this “mutation” is utilized to “guess” a new starting point to kick-start the whole process again. And finally the fitness function is used to select the “optimum” children to be used to regenerate the whole process all over again only if some predetermined optimum point has not been reached yet.

In the previous section, it is demonstrated that by “manually” adjusting the  $DWT^{-1}$  “g2” and “h2” affected the resultant reconstructed data. Using a GA, this step will now be accomplished “automatically” in the hopes of minimizing the quantization noise for images. Prior to this research, it was not known whether any academic, commercial, or military organization had attempted to use GAs to derive (or select and then optimize) alternative sets of “evolved” wavelet filter coefficients that perform better than standard wavelets for particular applications. Instead, memory-consuming look-up tables have historically been utilized by various DSP embedded processors. What is needed, especially in the military operations field, is a system that derives particular optimized filters in real time for a particular mission mode of operation (e.g., specifications) and background clutter (e.g., raw data). Such a system potentially negates the necessity of using large look-up tables stored in RAM or ROM. For this effort, the GA was utilized to “tweak” the least significant bits of preselected wavelet filter coefficients. The purpose of the fitness function was to lower, if possible, the quantization noise to some predetermined acceptable level. This new process is depicted in Figure 15 which shows the top-level key components of the GA/DWT solution.

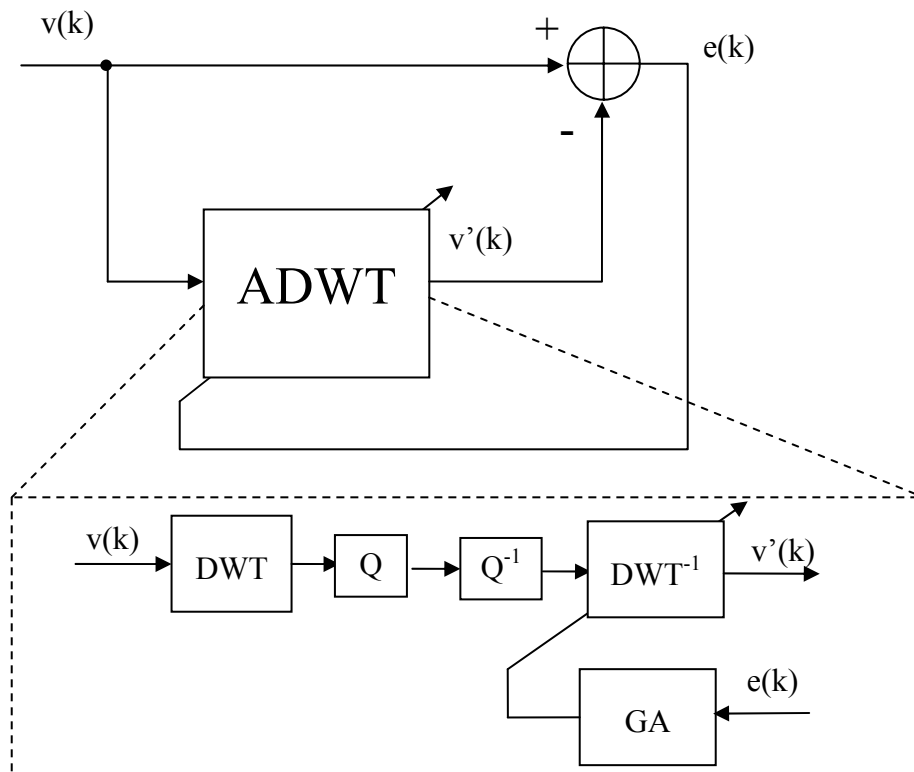


**Figure 15.** Basic GA Wavelet Optimization Experiment

Since encoding and decoding of the transmitted signal is not the main problem with image compression, neither of their algorithms will be utilized in these experiments. Only the quantization and DWT algorithms will be used to conduct all experiments.

Figure 16 is a detailed block diagram of the whole GA/DWT optimization process. It provides a detailed illustration of the evolutionary process it embodies.

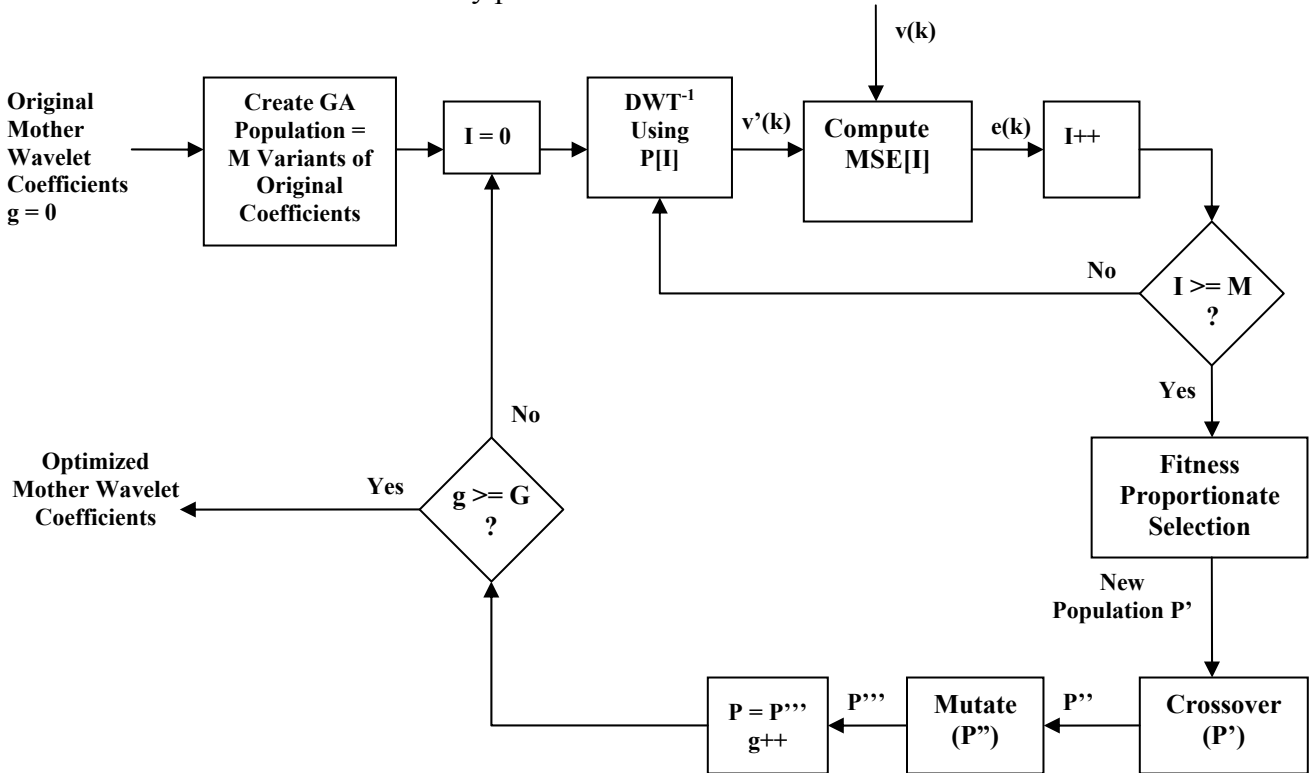


**Figure 16.** Detailed GA Wavelet Optimization Experiment.

Specifically, the above GA executes the following steps:

1. The initial population (generation 0) is represented by an array of  $M$  candidate solutions. Each candidate solution consists of a set of  $g_2$  and  $h_2$  values (as defined for the inverse wavelet transform). The GA begins by initializing the  $g_2$  and  $h_2$  values for each candidate solution to the values from the selected standard wavelet. Candidate solution 0 of generation 0 remains unchanged. For each of the remaining  $M-1$  candidate solutions, each of the  $g_2$  and  $h_2$  values is mutated by a small, random multiplicative factor (e.g., 0.99 or 1.02). Thus, generation 0 is initially seeded with one exact copy and  $M-1$  random perturbations of the selected standard wavelet (Garza and Maher 1999).
2. Next, the GA runs for a fixed number of generations ( $G$ ).
  - a) For each generation, the fitness of each candidate solution from current population is evaluated. For the vector and image data used in this investigation, fitness equals the summed magnitude of error between the original image and the image reconstructed using the wavelet coefficients that comprise the candidate solution.

- b) Tournament selection (Miller and Goldberg 1995) is then used to populate the next generation. With tournament selection, a predetermined number of individuals are randomly selected from the current generation, and the candidate solution with the best fitness value is copied into the next generation. This process is repeated M times in order to populate the next generation with M candidate solutions.
- c) Next, crossover is performed. Crossover pairs each member of the next generation with a second randomly selected individual. For this investigation, two crossover points (one for the  $g_2$  vector and one for the  $h_2$  vector) are identified, and the values at and below each crossover point are exchanged. Thus, the genetic composition of each child individual resulting from the crossover operation typically differs from that of both of the selected parent individuals.
- d) Next, mutation is randomly applied to a predetermined and small percentage of the coefficients in each of the candidate solutions in the next generation. For this problem, mutation consists of modifying a given coefficient by a small multiplicative factor, according to a selected Gaussian distribution. Samples of this are shown in Table 4 below.

**Table 4.** 20% Change in Daub4 Wavelets

| Factor | Mutation %    | Probability |
|--------|---------------|-------------|
| 1.01   | +1%           | 5%          |
| 1.02   | +2%           | 3%          |
| 1.03   | +3%           | 1%          |
| 0.97   | -3%           | 1%          |
| 0.98   | -2%           | 3%          |
| 0.99   | -1%           | 5%          |
| -1.0   | {sign change} | 1%          |

- e) Finally, the next generation simply replaces the current generation.
3. After repeating step 2 for  $G$  generations, the individual with the best fitness of the entire run is declared the solution. For this study, the best-of-run solution defines the set of  $g_2$  and  $h_2$  coefficients that minimizes the total error in the reconstructed signal.

By forcing generation 0 to include a verbatim copy of the standard wavelet, it guarantees that the solution evolved by the GA can do no worse than the standard wavelet. By seeding the initial population with randomly mutated copies of the selected standard wavelet, the evolutionary process becomes biased such that it focuses upon the immediately adjacent solution space. In addition, this GA can be modified such that the best solution from the current generation is copied into the next generation; this process guarantees that the best-of-generation fitness value will not worsen from one generation to the next.

## 8. RESULTS

Twelve tests were performed using 2-D image data. Each test was characterized by three factors:

1. The quantization factor: These tests used quantization values of 32 and 64.

2. The 2-D data being reconstructed: Several images commonly appearing in the wavelet literature were used, including “Airplane”, “Baboon”, “Barb”, “Boat”, “Couple”, “Fruits”, “Goldhill”, “Lenna”, “Park”, “Peppers”, “Susie”, and “Zelda”.
3. The selected standard wavelet: Wavelets used in these tests included the Daub4 (Daubechies 1988), 2/6 (Villasenor, Belzer, and Liao 1995), and 5/3 (Lin 1999) wavelets.

Each test consisted of two runs. The first run used the unmodified standard wavelet to reconstruct a selected image. The second run used a GA to evolve a new set of wavelet coefficients for a similarly structured wavelet. The result of each test compared the MSE and PSNR (Vetterli and Kovacevic 1995) of the evolved wavelet to the standard wavelet. These results compare the evolved coefficients to the standard coefficients, and state the percentage change in the magnitude of each coefficient.

**TEST RESULTS USING DAUB4:** The coefficients for the standard Daub4 inverse wavelet transform are shown below and their plots are shown in Figure 16 below.

$$h2 = \{0.482962913, 0.836516304, 0.224143868, -0.129409523\}$$

$$g2 = \{-0.129409523, -0.224143868, 0.836516304, -0.482962913\}$$

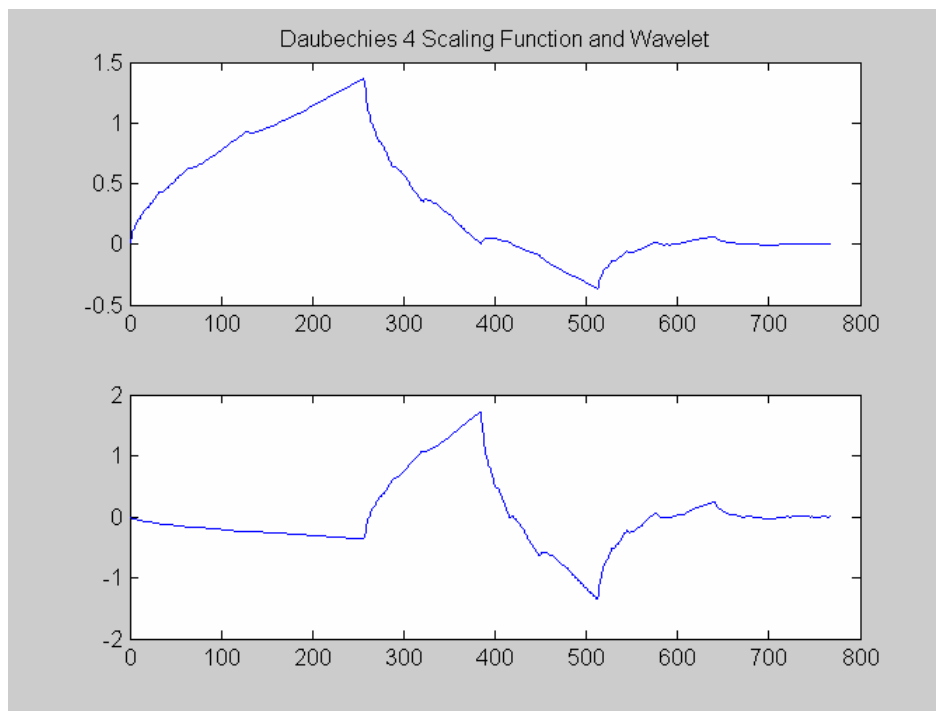


**Figure 16.** Standard Daub4 Scaling Function and Wavelet

**TEST 1:** Quantization = 32, Image = "Barb"

Daub4: MSE = 96.886522928 PSNR = 8.268169906

Evolved: MSE = 92.904186248 PSNR = 28.450450771

Percentage Change: MSE = -4.1103%% PSNR = +0.6648%

Evolved coefficients:  $h2' = \{0.46824367, 0.81126518, 0.23985918, -0.10537719\}$

$g2' = \{-0.17815653, -0.18627964, 0.78603730, -0.44936688\}$

Percentage change:  $\Delta h2 = \{-3.048\%, -3.019\%, +7.011\%, -18.571\%\}$

$\Delta g2 = \{+37.669\%, -16.893\%, -6.034\%, -6.034\%\}$

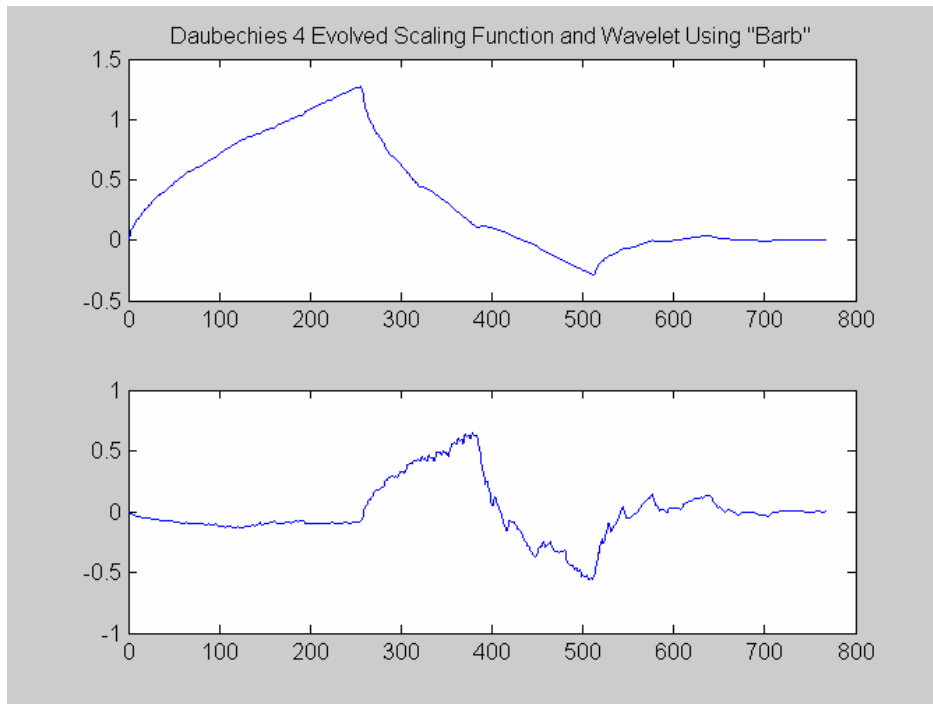


**Figure 17.** Resultant Daub4 Scaling Function and Wavelet with Coefficients Evolved Using "Barb" Image (Quantization = 32)

**TEST 2:** Quantization = 32, Image = "Boat"

|                    |                    |                     |
|--------------------|--------------------|---------------------|
| Daub4:             | MSE = 52.520229339 | PSNR = 30.927537470 |
| Evolved:           | MSE = 49.920497894 | PSNR = 31.148014526 |
| Percentage Change: | MSE = -4.9500%     | PSNR = +0.7129%     |

Evolved coefficients:  $h_2' = \{0.47813328, 0.80323285, 0.22855950, -0.09641626\}$

$g_2' = \{-0.20371400, -0.11414577, 0.76260869, -0.38425025\}$

Percentage Change:  $\Delta h_2 = \{-1.000\%, -3.979\%, +1.970\%, -29.495\%\}$

$\Delta g_2 = \{+57.418\%, -49.074\%, -8.835\%, -20.439\%\}$

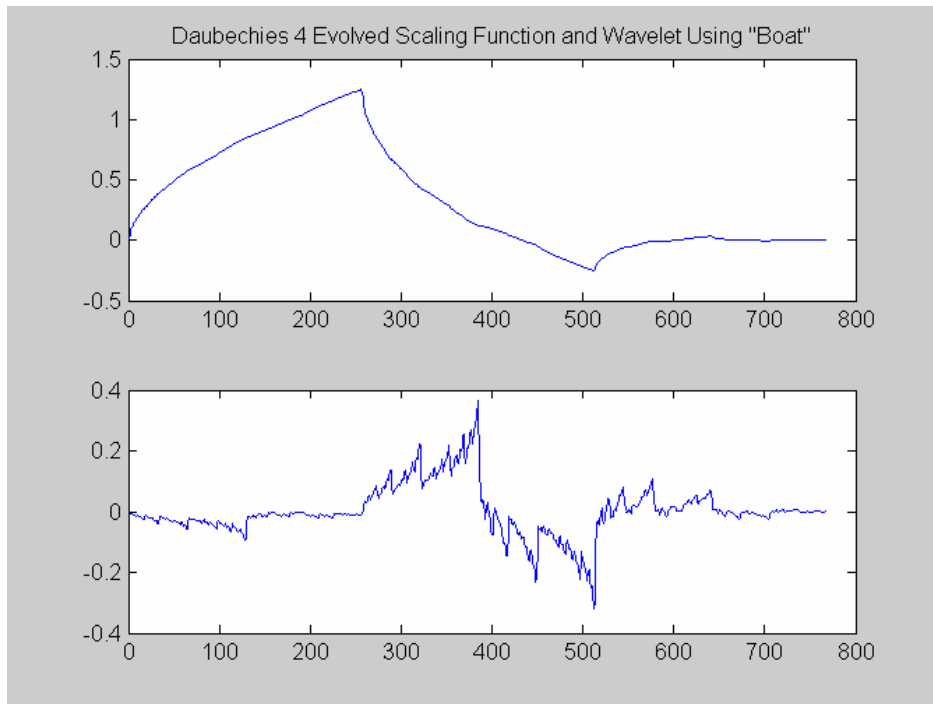


**Figure 18.** Resultant Daub4 Scaling Function and Wavelet with Coefficients Evolved Using "Boat" Image (Quantization = 32)

**TEST 3:** Quantization = 64, Image = "Couple"

Daub4: MSE = 155.96321105 PSNR = 26.200581927  
Evolved: MSE = 144.96800359 PSNR = 26.518082027  
Percentage Change: MSE = -7.0499% PSNR = +1.2118%

Evolved Coefficients:  $h2' = \{0.46393225, 0.78701072, 0.24254917, -0.07969529\}$   
 $g2' = \{-0.25739530, -0.07244071, 0.71684818, -0.34936503\}$   
Percentage Change:  $\Delta h2 = \{-3.940\%, -2.990\%, +8.211\%, -38.416\%\}$   
 $\Delta g2 = \{+98.900\%, -67.681\%, -14.306\%, -27.662\%\}$

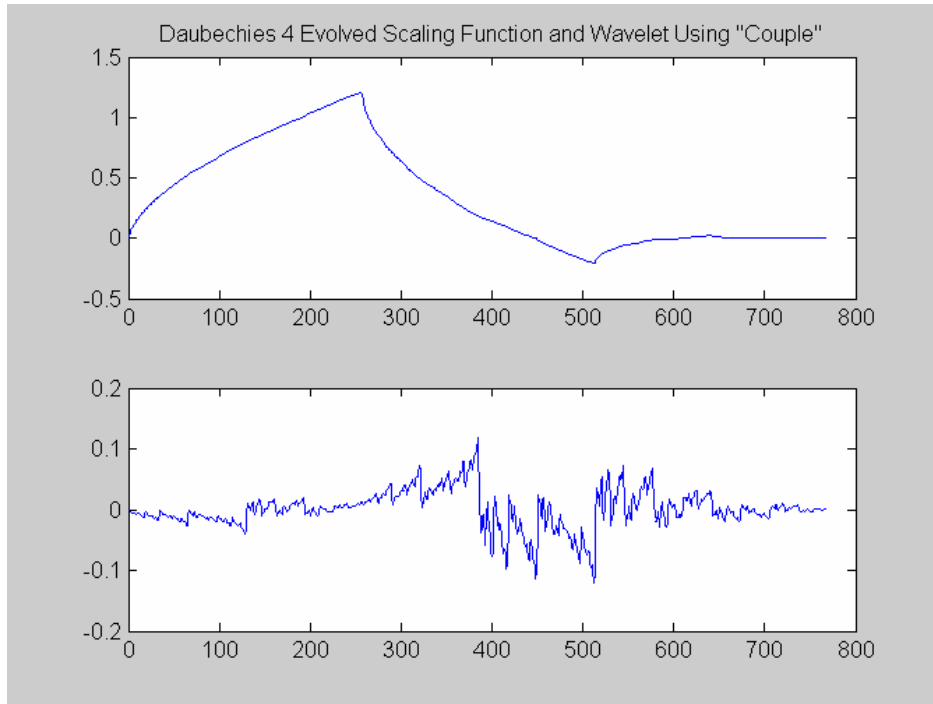


**Figure 19.** Resultant Daub4 Scaling Function and Wavelet with Coefficients Evolved Using "Couple" Image (Quantization = 64)

**TEST 4:** Quantization = 64, Image = "Fruits"

Daub4: MSE = 115.80363591 PSNR = 27.493581656  
Evolved: MSE = 110.45684432 PSNR = 27.698877292  
Percentage Change: MSE = -4.6171% PSNR = +0.7467%

Evolved Coefficients:  $h2' = \{0.45006297, 0.81150696, 0.25752134, -0.10514879\}$   
 $g2' = \{-0.15772549, -0.13019651, 0.71494264, -0.38877090\}$   
Percentage Change:  $\Delta h2 = \{-6.812\%, -2.990\%, +14.891\%, -18.747\%\}$   
 $\Delta g2 = \{+21.881\%, -41.914\%, -14.533\%, -19.503\%\}$

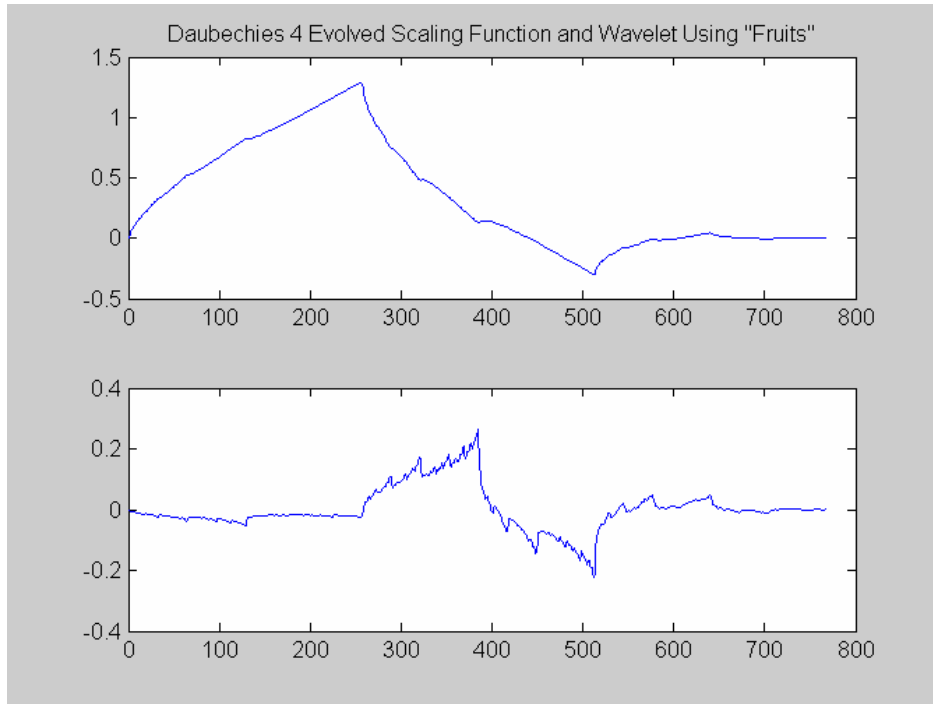


**Figure 20.** Resultant Daub4 Scaling Function and Wavelet with Coefficients Evolved Using "Fruits" Image (Quantization = 64)

## **SUMMARY OF RESULTS OF TESTS1-4 USING DAUB4 WAVELETS:**

Average Improvement, MSE: 5.1818%

Average Improvement, PSNR: 0.8341%

These results indicate that the GA was capable of evolving a set of real-valued coefficients that consistently outperformed a similarly structured Daub4 wavelet using standard wavelet coefficients. As a sample of one of these results, images before and after the transformation conducted for “TEST3” are shown in Figures 21-23. Close inspection of Figure 23 reveals minor improvements over the image shown in Figure 22 which was reconstructed via the standard Daub4 wavelet.



**Figure 21.** The Original “Couple” Image



**Figure 22.** “Couple” Reconstructed via the Standard Daub4 Wavelet (Quantization = 64)



**Figure 23.** “Couple” Reconstructed via an Evolved Wavelet (Quantization = 64).

**RESULTS USING 2/6 (TS) MOTHER WAVELETS:** The coefficients for the standard TS inverse wavelet transform are shown below and their plots are shown in Figure 24.

$$h2 = \{-0.088388, 0.088388, 0.707107, 0.707107, 0.088388, -0.088388\}$$
$$g2 = \{-0.70710678, 0.70710678\}$$

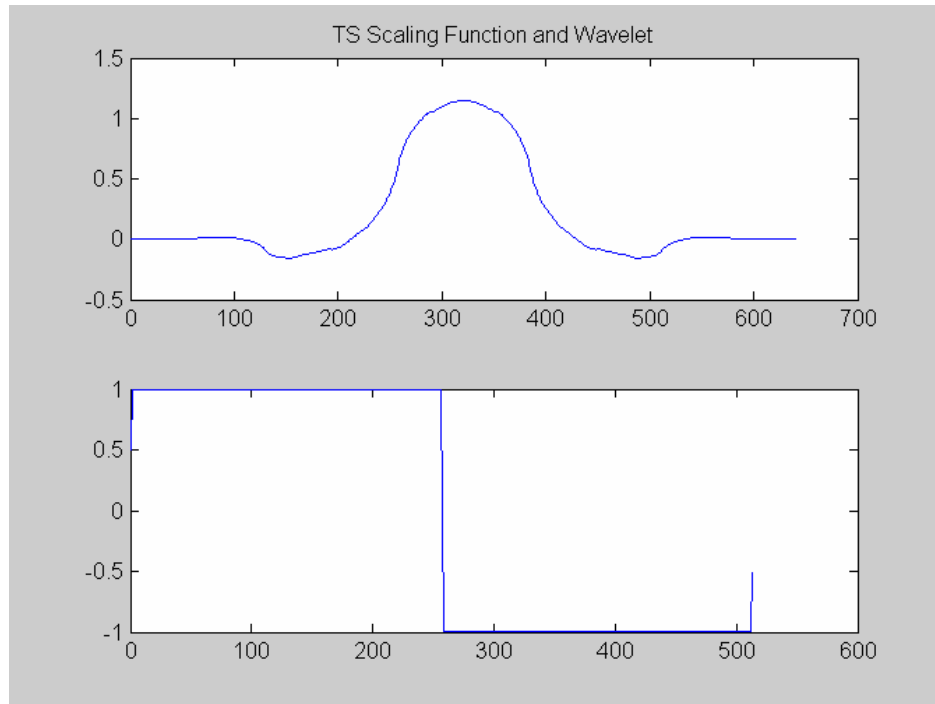


**Figure 24.** Standard TS Scaling Function and Wavelet

**TEST 5:** Quantization = 32, Image = "Goldhill"

TS: MSE = 55.693927764 PSNR = 30.672725136

Evolved: MSE = 52.678527832 PSNR = 30.914467313

Percentage Change: MSE = -5.4142% PSNR = +0.7881%

Evolved Coefficients:  $h_2' = \{-0.07478096, 0.11289088, 0.68569361, 0.66566063, 0.09555358, -0.07139243\}$

$g_2' = \{-0.61834085, 0.61191382\}$

Percentage Change:  $\Delta h_2 = \{-15.395\%, +27.075\%, -3.028\%, -5.861\%, +8.107\%, -19.228\%\}$

$\Delta g_2 = \{-12.553\%, -12.331\%\}$

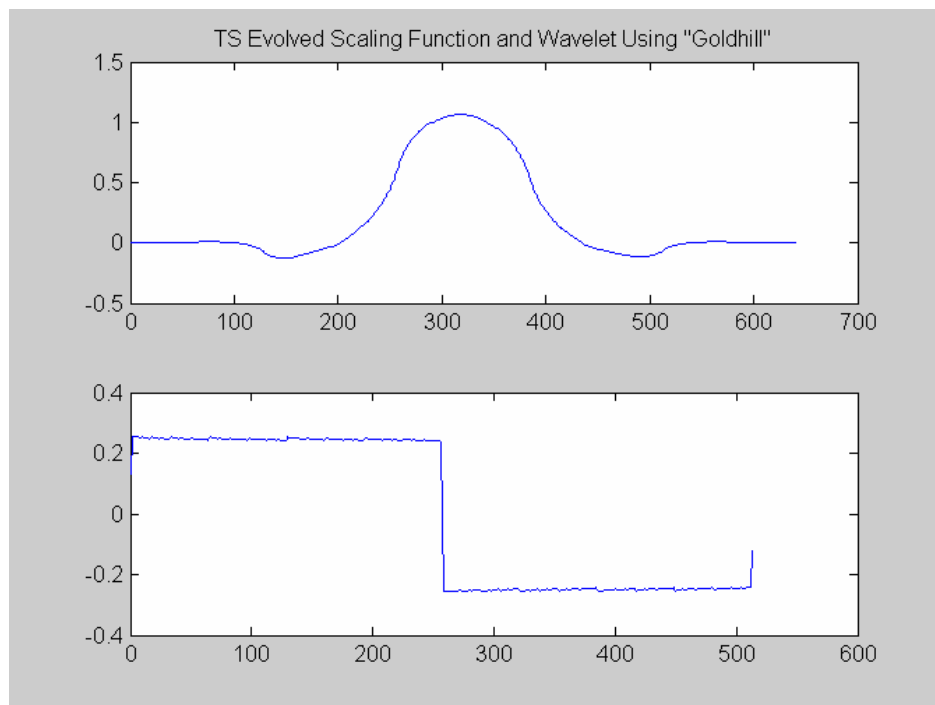


**Figure 25.** Resultant TS Scaling Function and Wavelet with Coefficients Evolved Using "Goldhill" Image (Quantization = 32)

**TEST 6:** Quantization = 32, Image = "Park"

TS: MSE = 68.487875620 PSNR = 29.774666655

Evolved: MSE = 65.506455739 PSNR = 29.967962585

Percentage Change: MSE = -4.3532% PSNR = +0.6492%

Evolved Coefficients:  $h2' = \{-0.07336637, 0.11436371, 0.67917624,$   
 $0.67238448, 0.10247711, -0.07791956\}$

$g2' = \{-0.65717215, 0.66505474\}$

Percentage Change:  $\Delta h2 = \{-16.995\%, +29.388\%, -3.950\%,$   
 $-4.911\%, +15.940\%, -11.844\%\}$

$\Delta g2 = \{-7.062\%, -5.947\%\}$

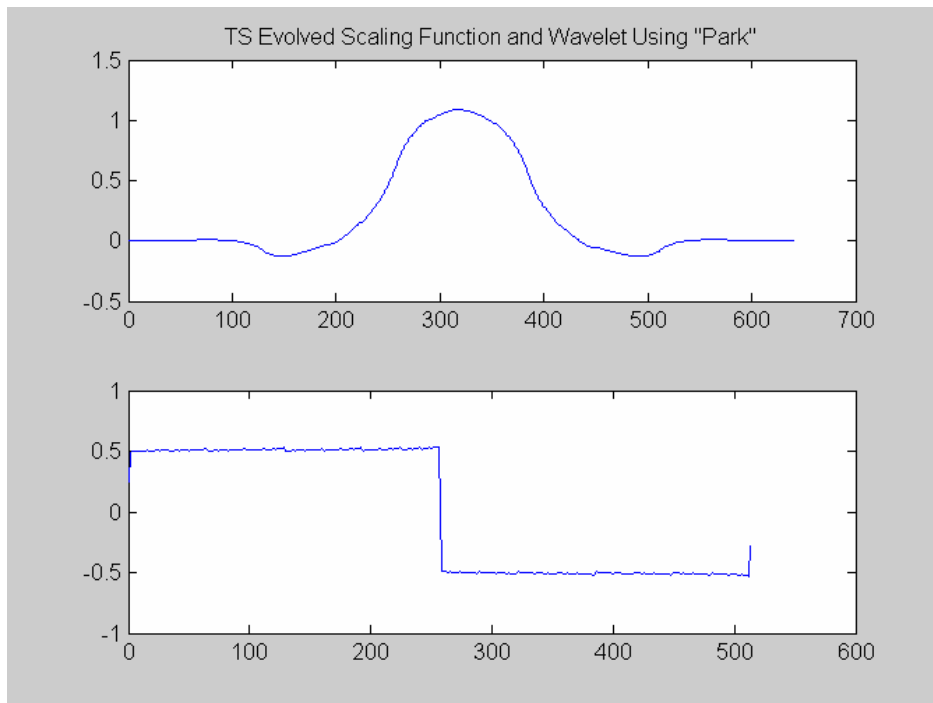


**Figure 26.** Resultant TS Scaling Function and Wavelet with Coefficients Evolved Using "Park" Image (Quantization = 32)

**TEST 7:** Quantization = 64, Image = "Peppers"

TS: MSE = 124.52128283 PSNR = 27.178367746

Evolved: MSE = 112.26459054 PSNR = 27.628375641

Percentage Change: MSE = -9.8431% PSNR = +1.6558%

Evolved Coefficients:  $h_2' = \{-0.06290282, 0.12320526, 0.66566063,$   
 $0.63949490, 0.10331971, -0.05645800\}$

$g_2' = \{-0.67870071, 0.78100922\}$

Percentage Change:  $\Delta h_2 = \{-28.946\%, +39.391\%, -5.861\%,$   
 $-9.562\%, +16.893\%, -36.125\%\}$

$\Delta g_2 = \{-4.107\%, +10.451\%\}$

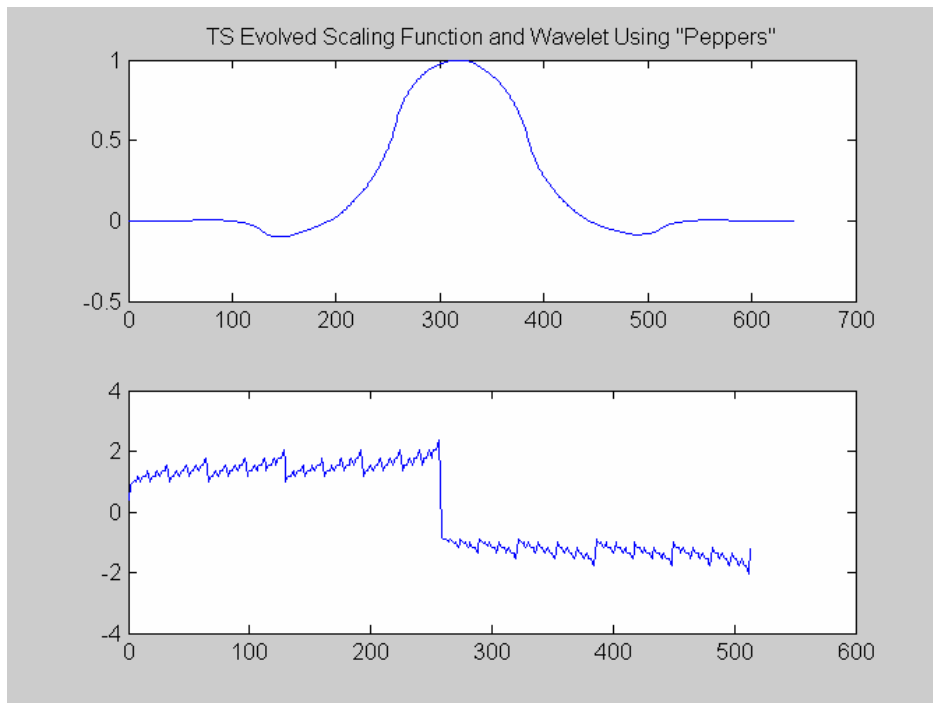


**Figure 27.** Resultant TS Scaling Function and Wavelet with Coefficients Evolved Using "Peppers" Image (Quantization = 64)

**TEST 8:** Quantization = 64, Image = "Susie"

TS: MSE = 133.22735341 PSNR = 26.884869602

Evolved: MSE = 118.87997182 PSNR = 27.379716673

Percentage Change: MSE = -10.7691% PSNR = +1.8406%

Evolved Coefficients:  $h_2' = \{-0.06581485, 0.12938192, 0.66566063,$   
 $0.63309995, 0.10846400, -0.05439425\}$

$g_2' = \{-0.61788622, 0.72802296\}$

Percentage Change:  $\Delta h_2 = \{-25.539\%, +46.380\%, -5.861\%,$   
 $-10.466\%, +22.713\%, -38.460\%\}$

$\Delta g_2 = \{-12.618\%, +2.958\%\}$

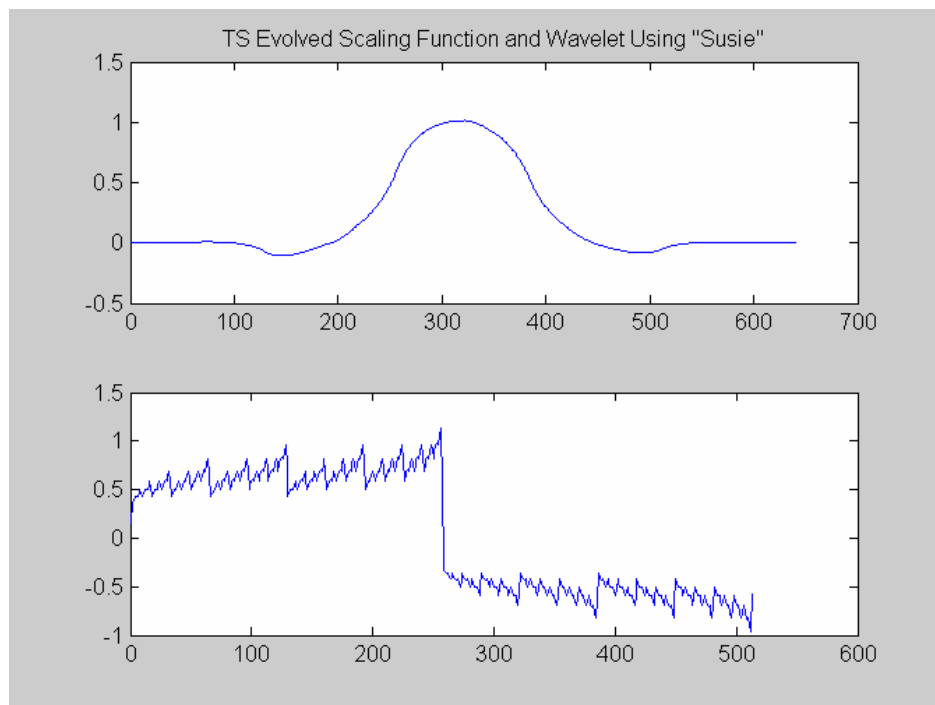


**Figure 28.** Resultant TS Scaling Function and Wavelet with Coefficients Evolved Using "Susie" Image (Quantization = 64)

## **SUMMARY OF RESULTS OF TESTS 5-8 USING TS WAVELETS:**

Average Improvement, MSE: 7.5949%

Average Improvement, PSNR: 1.2334%

These results indicate that our GA was capable of evolving a set of real-valued coefficients that consistently outperformed a similarly structured TS wavelet using standard wavelet coefficients. Improvements in both the MSE and the PSNR for the TS wavelet were consistently greater than the corresponding improvement for the Daub4 wavelet seen in the first four tests.

The sample image results for “TEST 8” are shown in Figures 29-31. As can be seen, slight improvements in shading and detail are visible in Figure 31 as compared the image reconstructed using the standard TS wavelet shown in Figure 30.



**Figure 29.** The Original “Susie” Image



**Figure 30.** “Susie” Reconstructed via the Standard TS Wavelet (Quantization = 64).



**Figure 31.** “Susie” Reconstructed via an Evolved Wavelet (Quantization = 64).

**RESULTS USING 5/3 (FT) MOTHER WAVELETS:** The coefficients for the standard FT inverse wavelet transform are shown below along with their corresponding plots in Figure 32.

$$h2 = \{0.353553, 0.70710678, 0.353553\}$$
$$g2 = \{-0.176777, -0.353553, 1.060660, -0.353553, -0.176777\}$$

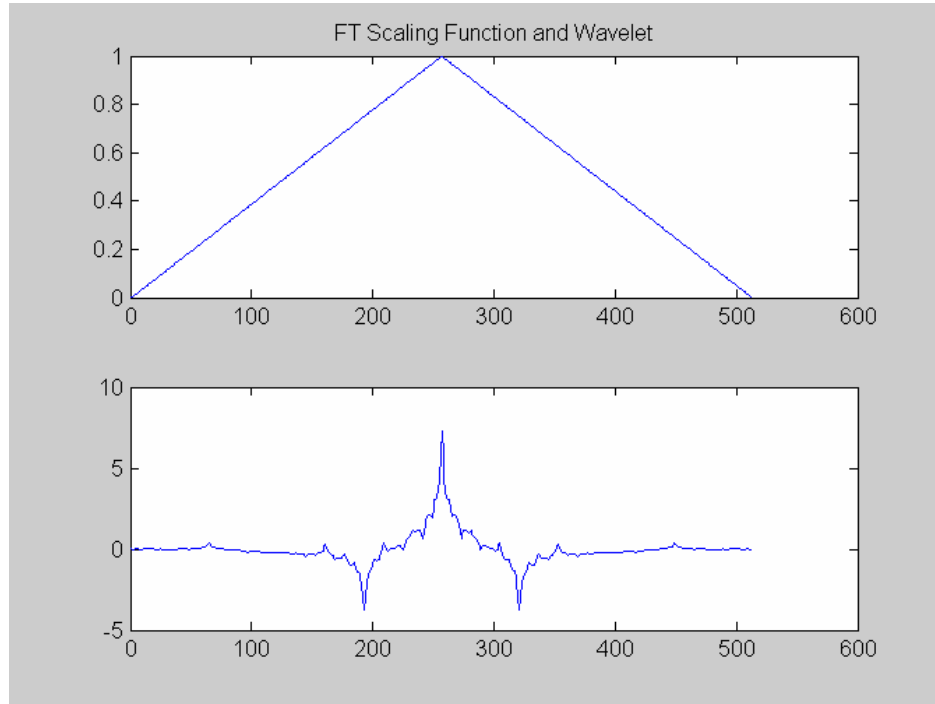


**Figure 32.** Standard FT Scaling Function and Wavelet

**TEST 9:** Quantization = 32, Image = "Airplane"

FT: MSE = 35.743078867 PSNR = 32.598884014

Evolved: MSE = 35.453097025 PSNR = 32.634261816

Percentage Change: MSE = -0.8113% PSNR = +0.1085%

Evolved Coefficients:  $h2' = \{0.35708853, 0.70703607, 0.35001747\}$

$g2' = \{-0.22535310, -0.34301712, 1.09116094,$   
 $-0.35623248, -0.22755308\}$

Percentage Change:  $\Delta h2 = \{+1.000\%, -0.010\%, -1.000\%\}$

$\Delta g2 = \{+27.479\%, -2.980\%, +2.875\%,$   
 $+0.758\%, +28.723\%\}$

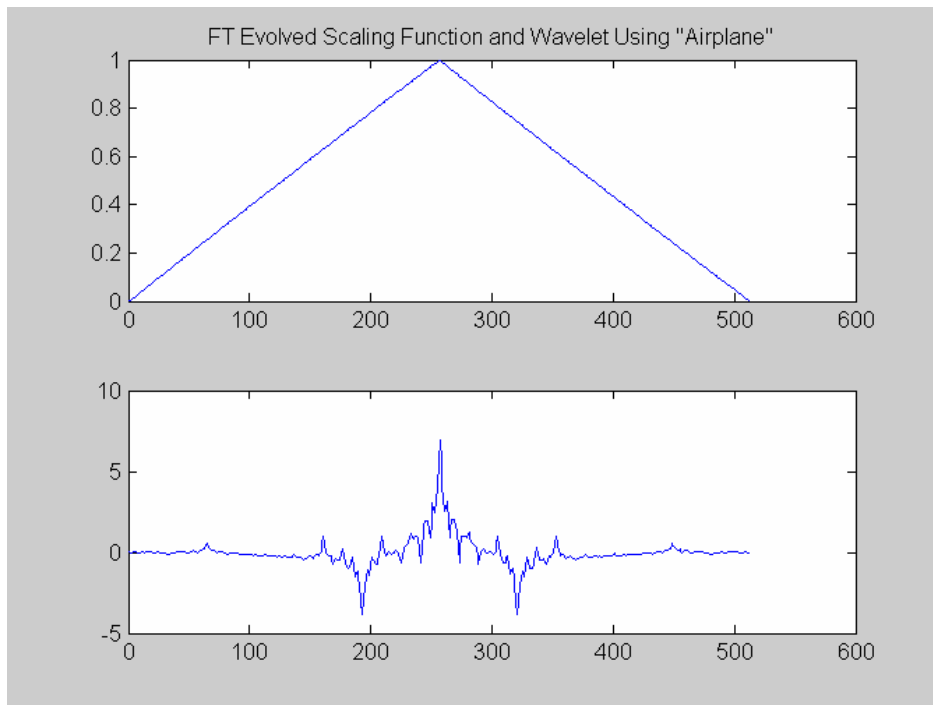


**Figure 33.** Resultant FT Scaling Function and Wavelet with Coefficients Evolved Using "Airplane" Image (Quantization = 32)

**TEST 10:** Quantization = 32, Image = “Baboon”

FT: MSE = 113.09576543 PSNR = 27.596340166

Evolved: MSE = 111.85707219 PSNR = 27.644169131

Percentage Change: MSE = -1.0953% PSNR = +0.1733%

Evolved Coefficients:  $h2' = \{0.35001747, 0.70682398, 0.35708853\}$

$g2' = \{-0.20626139, -0.31293066, 0.99595579$

$-0.31273186, -0.20463438\}$

Percentage Change:  $\Delta h2 = \{-1.000\%, -0.040\%, 1.000\%\}$

$\Delta g2 = \{+16.679\%, -11.490\%, -6.100\%,$

$-11.546\%, +15.758\%\}$

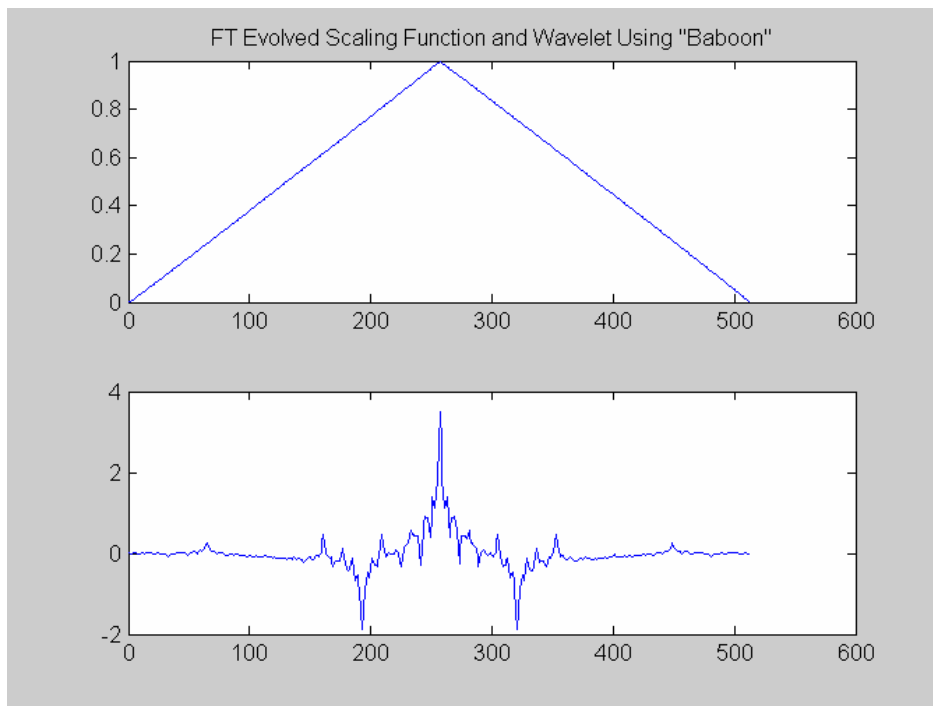


**Figure 34.** Resultant FT Scaling Function and Wavelet with Coefficients Evolved Using “Baboon” Image (Quantization = 32)

**TEST 11:** Quantization = 64, Image = "Lenna"

FT: MSE = 140.01809946 PSNR = 26.668961823

Evolved: MSE = 139.92291514 PSNR = 26.671915162

Percentage Change: MSE = -0.0680% PSNR = +0.0111%

Evolved Coefficients:  $h2' = \{0.34627481, 0.70689467, 0.36051517\}$

$g2' = \{-0.26215020, -0.26897337, 0.77367288, -0.33877071, -0.21314989\}$

Percentage Change:  $\Delta h2 = \{-2.059\%, -0.030\%, +1.969\%\}$

$\Delta g2 = \{+48.294\%, -23.923\%, -27.057\%, -4.181\%, +20.576\%\}$

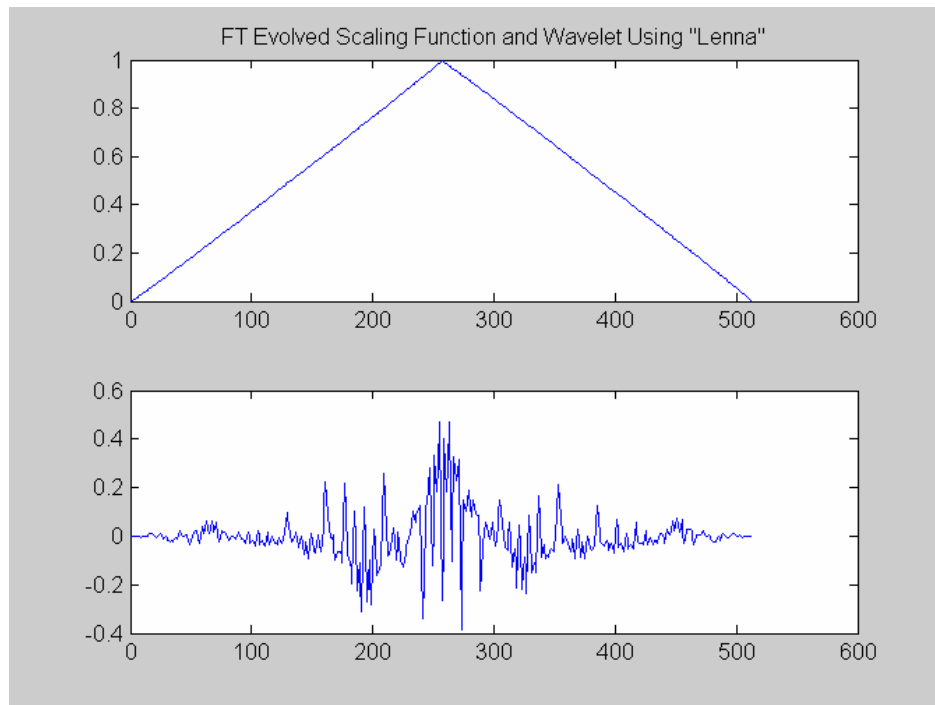


**Figure 35.** Resultant FT Scaling Function and Wavelet with Coefficients Evolved Using "Lenna" Image (Quantization = 64)

**TEST 12:** Quantization = 64, Image = "Zelda"

FT: MSE = 111.79914855 PSNR = 27.646418648

Evolved: MSE = 110.98122024 PSNR = 27.678308652

Percentage Change: MSE = -0.7316% PSNR = +0.1153%

Evolved Coefficients:  $h_2' = \{0.33251660, 0.70668262, 0.37494296\}$

$g_2' = \{-0.18713481, -0.36715097, 0.85353342,$   
 $-0.28083948, -0.44643196\}$

Percentage Change:  $\Delta h_2 = \{-5.950\%, -0.060\%, +6.050\%\}$

$\Delta g_2 = \{+5.859\%, +3.846\%, -19.528\%,$   
 $-20.567\%, +152.540\%\}$

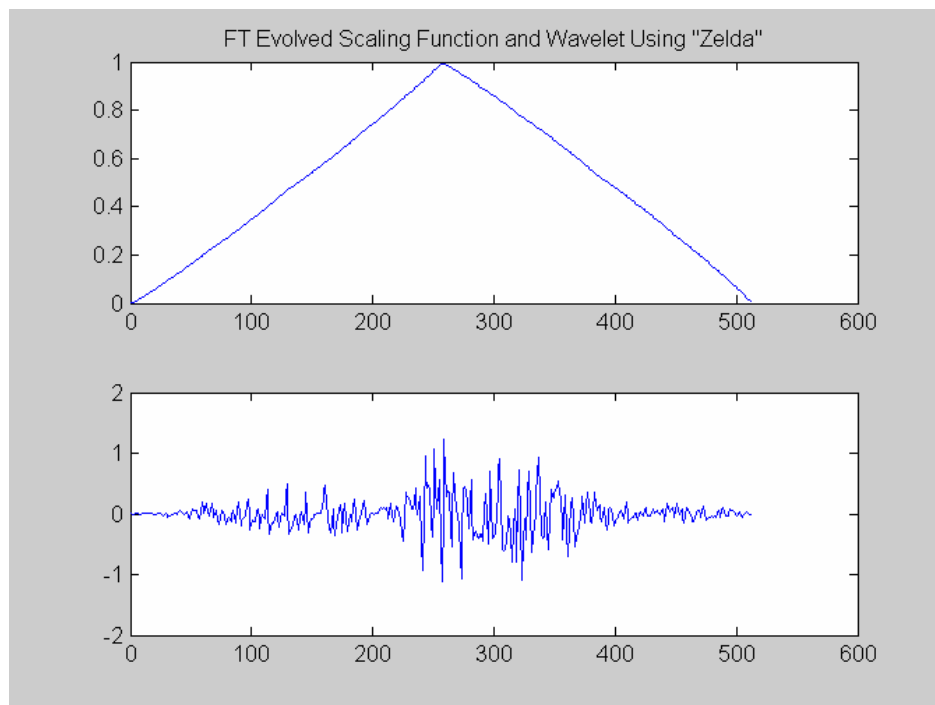


**Figure 36.** Resultant FT Scaling Function and Wavelet with Coefficients Evolved Using "Zelda" Image (Quantization = 64)

## **SUMMARY OF RESULTS OF TESTS 9-12 USING FT WAVELETS:**

Average Improvement, MSE: 0.6766%

Average Improvement, PSNR: 0.1021%

These results indicate that the GA is again capable of evolving a set of real-valued coefficients. Unfortunately in this case the percentage of improvement is much smaller than previously noted for the Daub4 and 2/6 wavelets.

Sample image results for “TEST 10” are shown in Figures 37-39. As can be seen, differences between Figures 38 and 39 are too small to be perceived by the naked eye.

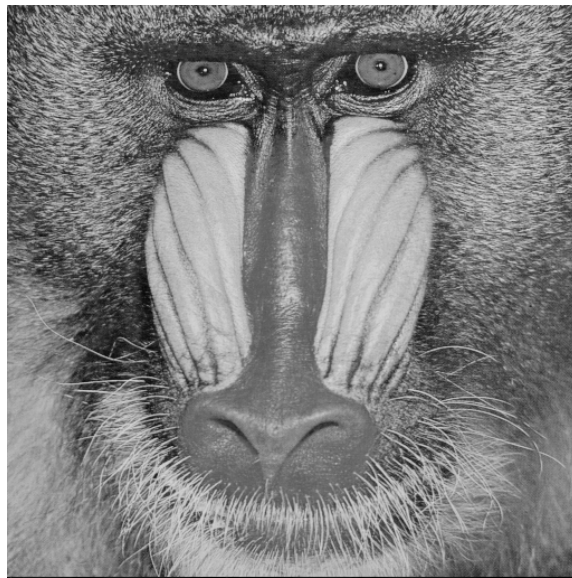


**Figure 37.** The Original “Baboon” Image

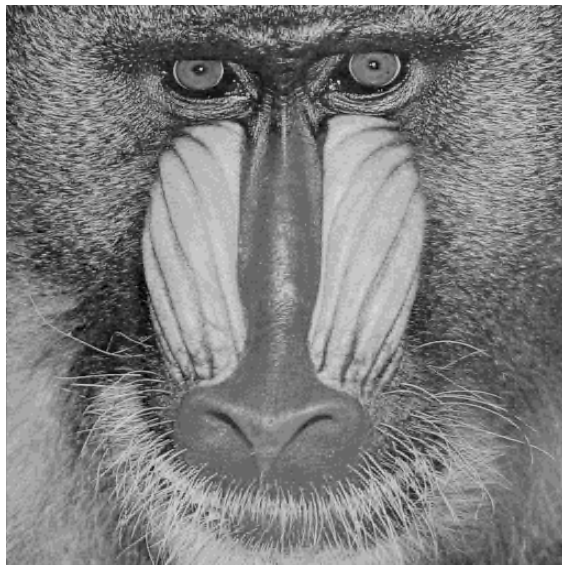


**Figure 38.** “Baboon” Reconstructed via the Standard FT Wavelet (Quantization = 32).

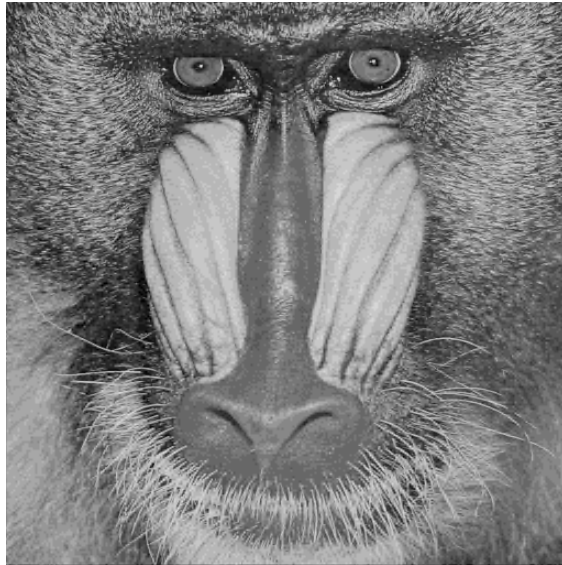


**Figure 39.** “Baboon” Reconstructed via an Evolved Wavelet (Quantization = 32).

### **OVERALL RESULTS (ALL 12 TESTS):**

Average Improvement, MSE: 4.4844%  
Average Improvement, PSNR: 0.7232%

## **9. CONCLUSION**

Prior to this study, it was believed that not too many active wavelet researchers would have believed it possible to systematically modify the filter coefficients of standard, “off-the-shelf” wavelets in the hopes of reducing MSE and improving PSNR. However, the results of this effort conclusively illustrate that wavelet filter coefficients can be optimized via a GA. This process improves upon the performance of similarly structured standard wavelets (such as the Daub4, TS, and FT wavelets used in these tests) for lossy image reconstruction applications.

## **10. APPLICATIONS OF THE NEW TECHNOLOGY AND FUTURE RESEARCH**

Although most of the incremental improvements summarized in the document are at best barely detectable to the naked eye, they nevertheless appear to have established a basic method that may ultimately lead to significant enhancement of modern image reconstruction technology. The approach established by this investigation promises improvement upon state of the art wavelet decompression techniques for a wide range of applications, including audio denoising (Schremmer, Haenselmann, and Bömers 2001), sea clutter noise reduction for radar proximity fusing (Noel and Szu 1998), signal compression (Saito 1994), object detection (Zhu and Schwartz 2002), fingerprint compression (Bradley, Brislawn, and Hopper 1993), image denoising (Chang, Yu, and Vetterli 1998), image enhancement (Wang, Wu, Castleman, and Xiong 2001), image recognition (Schilling, Cosman, and Berry 1998), and speech recognition (Long and Datta 1998).

This research demonstrates that a GA can evolve coefficients for the inverse wavelet transform that reduced MSE in comparison to a standard wavelet transform of the same image. The question of whether a single wavelet could be evolved that outperforms standard wavelets for a *specific class of images* (e.g., satellite images), or even for *all possible images*, has yet to be addressed. Future efforts will attempt to evolve a “super wavelet” capable of producing higher fidelity reconstructions of transformed, quantized images than any previously identified wavelet.

This research evolved coefficients of inverse wavelet transforms that minimize the total MSE in reconstructed images that had originally been (forward) transformed by wavelets utilizing standard coefficients. It is possible, however, that the overall performance of our evolved wavelet reconstruction system could be further improved by *simultaneously evolving coefficients for the forward wavelet transform*. In effect, this effort would attempt to evolve sets of coefficients for matching forward and inverse transforms under conditions subject to quantization error. Future research should therefore investigate the possibility of simultaneously evolving coefficients for both the forward and inverse wavelet transform.

The GA developed for this study uses an initial population that is created by randomly mutating copies of a selected standard wavelet. This process biased the search, causing the GA to focus primarily upon the solution space immediately adjacent to the standard wavelet. Hence, the evolved wavelet is typically very similar to the standard wavelet. It is as yet unknown whether the evolutionary process could locate optimized solutions in entirely new and previously unexploited neighborhoods of the solution space. Future work will therefore include attempts to evolve wavelets without imparting any bias to the search process.

Noise (Fante 1988) refers to the introduction of any undesired change in the information content of a signal during transmission. Thresholding (the removal of wavelet coefficients whose magnitude is less than a predetermined noise threshold) is often used to eliminate random noise (Donoho and Johnstone 1994). Various wavelet-based methods have also been shown to be highly effective (Donoho 1993). In many situations, however, a transformed signal is likely to contain several low-energy values that may make an important contribution to an accurate reconstruction of the original signal. If these values lie below the noise threshold, denoising will remove them from the transformed signal, and subsequent reconstruction may produce an unsatisfactory approximation of the original signal (Malfait 1996). Although the current research effort focused primarily upon the elimination of error due to the quantization process, future research may expand upon our results by developing novel approaches to noise reduction in signal and image processing applications.

The JPEG 2000 image compression standard (Charrier, Cruz, and Larsson 1999) uses wavelet technology to compress and subsequently reconstruct images. It is possible that the wavelets optimized during this study could replace standard wavelets for lossy image compression applications in the next JPEG release. Future research should specifically address the JPEG standard and identify scenarios in which evolved wavelets could potentially outperform standard JPEG wavelets. A similar approach may also be applied to other wavelet-based standards.

## 11. ACKNOWLEDGMENT

This work was sponsored by the AFOSR/NM Optimization and Discrete Mathematics office. The authors of this paper would like to thank **Lt. Col. Juan Vasquez**, the AFOSR/NM program manager, for his guidance and support during this effort.

## 12. BIBLIOGRAPHY

Bradley, J. N., C. M. Brislawn, and T. Hopper 1993. The FBI Wavelet-Scalar Quantization Standard for Grey-Scale Fingerprint Compression, *Visual Information Processing II*, Vol. 1961: 293-304, *Proceedings of the SPIE*, Orlando, FL.

Burrus, C. S., R. A. Gopinath, and H. Guo 1998. *Introduction to Wavelets and Wavelet Transforms: A Primer*, Prentice-Hall.

Chang, S. 1995. *Image Interpolation Using Wavelet-Based Edge Enhancement and Texture Analysis*, Master's Thesis, University of California at Berkeley.

Chang, G., B. Yu, and M. Vetterli 1998. Spatially adaptive wavelet thresholding based on context modeling for image denoising, *IEEE Transactions on Image Processing*.

Charrier, M., D. S. Cruz, and M. Larsson 1999. JPEG2000, the Next Millennium Compression Standard for Still Images, *IEEE International Conference on Multimedia Computing and Systems*, 1: 131-132.

Cooley, J. W. and J. W. Tukey 1965. An Algorithm for the machine calculation of complex Fourier series, *Mathematics of Computation*, 19: 297-301.

Daubechies, I. 1988. Orthonormal Bases of Compactly Supported Wavelets, *Communications of Pure and Applied Mathematics*, 41:909-996.

Daubechies, I. 1992. *Ten Lectures on Wavelets*, SIAM.

Davis, G. M. and A. Nosratinia 1998. Wavelet-based Image Coding: An Overview, *Applied and Computational Control, Signals, and Circuits*, 1(1).

Donoho, D. 1993. Nonlinear Wavelet Methods for Recovery of Signals, Densities, and Spectra from Indirect and Noisy Data, in Daubechies, I. (Ed.), *Different Perspectives on Wavelets*, AMS.

Donoho, D. and I. Johnstone 1994. Ideal Spatial Adaptation via Wavelet Shrinkage, *Biometrika*, 81: 425-455.

Fante, R.L., 1988. *Signal Analysis and Estimation: an Introduction*, John Wiley.

Garza, A. G. and M. L. Maher 1999. An Evolutionary Approach to Case Adaptation, *Third International Conference on Case-Based Reasoning (ICCBR'99)*, Springer-Verlag.

- Goldberg, D. E. 1989. *Genetic Algorithms in Search, Optimization, and Machine Learning*, Addison-Wesley.
- Graps, A. 1995. An Introduction to Wavelets, *IEEE Computational Science and Engineering*, 2(2), IEEE.
- Haar, A. 1910. Zur Theorie der orthogonalen Funktionensysteme, *Mathematische Annalen*, 69: 331-371.
- Holland, J. 1975. *Adaptation in Natural and Artificial Systems*, University of Michigan Press.
- Lin, C. 1999. *Time and Space Efficient Wavelet Transform for Real-Time Applications*, doctoral dissertation, The Ohio State University, 161-2.
- Long, C. J. and S. Datta 1998. Discriminant Wavelet Basis Construction for Speech Recognition, *5th International Conference on Spoken Language Processing (ICSLP 98)*, 3: 1047-1050.
- Malfait, M. 1996. Using Wavelets to Suppress Noise in Biomedical Images, in Aldroubi, A. and M. Unser (Eds.), *Wavelets in Medicine and Biology*, CRC Press.
- Mallat, S. 1989. A Theory for Multiresolution Signal Decomposition: The Wavelet Decomposition, *IEEE Transactions on Pattern Analysis and Machine Intelligence*, 11: 674-693.
- Mallat, S. 1998. *A Wavelet Tour of Signal Processing*, Academic Press.
- Miller, B. L. and D. E. Goldberg 1995. Genetic Algorithms, Tournament Selection, and the Effects of Noise, *Complex Systems*, 9:193-212.
- Noel, S. and H. Szu, 1998. Wavelets and Neural Networks for Radar, *Progress in Unsupervised Learning of Artificial Neural Networks and Real-World Applications*, Russian Academy of Nonlinear Sciences, ISBN 0-620-23629-9.
- Rajoub, B. A. 2002. An Efficient Coding Algorithm for the Compression of ECG Signals Using the Wavelet Transform, *IEEE Transactions on Biomedical Engineering*, 49(4): 355-362.
- Saha, S. 2000. Image Compression – from DCT to Wavelets: A Review, *ACM Crossroads*, ACM.
- Saito, N. 1994. Simultaneous Noise Suppression and Signal Compression using a Library of Orthonormal Bases and the Minimum Description Length Criterion, in Foufoula-Georgiou, E. and P. Kumar (Eds.), *Wavelets in Geophysics, Wavelet Analysis and Its Applications Vol. 4*, Academic Press.
- Schilling, D., P. Cosman, and C. Berry 1998. Image Recognition in Single-scale and Multiscale Decoders, *Proceedings of the 32nd Asilomar Conference on Signals, Systems, and Computers*, IEEE Computer Society Press.

Schremmer, C., T. Haenselmann, and F. Bömers 2001. A Wavelet Based Audio Denoiser, *IEEE International Conference on Multimedia and Expo (ICME) 2001*, 145-148.

Shannon, C. E. and W. Weaver 1964. *The Mathematical Theory of Communication*, The University of Illinois Press.

Stein, E. M. and G. Weiss 1971. *Introduction to Fourier Analysis in Euclidean Spaces*, Princeton Mathematical Series 32, Princeton University Press.

Vaidyanathan, P. P. 1992. *Multirate Systems and Filter Banks*, Prentice-Hall.

Vetterli, M. and J. Kovacevic 1995. *Wavelets and Subband Coding*, Prentice-Hall.

Villasenor, J., B. Belzer, and J. Liao 1995. Wavelet filter evaluation for image compression, *IEEE Transactions on Image Processing*, 4(8): 1053-1060.

Walker, J. S. 1999. *A Primer on Wavelets and their Scientific Applications*, CRC Press.

Wang, Y., Q. Wu, K. R. Castleman, and Z. Xiong 2001. Image Enhancement Using Multiscale Oriented Wavelets, *Proceedings, IEEE International Conference on Image Processing (ICIP'01)*, Thessalonica, Greece.

Zhu, Y. and S. Schwartz 2002. Discriminant Analysis and Adaptive Wavelet Feature Selection for Statistical Object Detection, *Proceedings, 16th International Conference on Pattern Recognition (ICPR'02)*, 4: 40086-40089, IEEE.